

A Second-Generation (44-Channel) Suprachoroidal Retinal Prosthesis: Interim Clinical Trial Results

Matthew A. Petoe^{1,2}, Samuel A. Titchener^{1,2}, Maria Kolic³, William G. Kentler⁴, Carla J. Abbott^{3,5}, David A. X. Nayagam^{1,6}, Elizabeth K. Baglin³, Jessica Kvensakul^{1,2}, Nick Barnes⁷, Janine G. Walker^{7,8}, Stephanie B. Epp¹, Kiera A. Young³, Lauren N. Ayton^{3,5,9}, Chi D. Luu^{3,5}, and Penelope J. Allen^{3,5}, for the Bionics Institute and Centre for Eye Research Australia Retinal Prosthesis Consortium

¹ Bionics Institute, East Melbourne, Victoria, Australia

² Medical Bionics Department, University of Melbourne, Melbourne, Victoria, Australia

³ Centre for Eye Research Australia, Royal Victorian Eye and Ear Hospital, Melbourne, Victoria, Australia

⁴ Department of Biomedical Engineering, University of Melbourne, Melbourne, Victoria, Australia

⁵ Ophthalmology, Department of Surgery, University of Melbourne, Melbourne, Victoria, Australia

⁶ Department of Pathology, University of Melbourne, St. Vincent's Hospital, Victoria, Australia

⁷ Research School of Engineering, Australian National University, Canberra, Australian Capital Territory, Australia

⁸ Health & Biosecurity, CSIRO, Canberra, Australian Capital Territory, Australia

⁹ Department of Optometry and Vision Sciences, University of Melbourne, Australia

Correspondence: Penelope J. Allen, Centre for Eye Research Australia, Level 7 Peter Howson Wing, 32 Gisborne St, East Melbourne, Victoria 3002, Australia. e-mail: pjallen@melbournere retina.com.au

Received: October 6, 2020

Accepted: August 24, 2021

Published: September 28, 2021

Keywords: retinal prosthesis; suprachoroidal; low vision

Citation: Petoe MA, Titchener SA, Kolic M, Kentler WG, Abbott CJ, Nayagam DAX, Baglin EK, Kvensakul J, Barnes N, Walker JG, Epp SB, Young KA, Ayton LN, Luu CD, Allen PJ. A second-generation (44-channel) suprachoroidal retinal prosthesis: Interim clinical trial results. *Transl Vis Sci Technol.* 2021;10(10):12, <https://doi.org/10.1167/tvst.10.10.12>

Purpose: To report the initial safety and efficacy results of a second-generation (44-channel) suprachoroidal retinal prosthesis at 56 weeks after device activation.

Methods: Four subjects, with advanced retinitis pigmentosa and bare-light perception only, enrolled in a phase II trial (NCT03406416). A 44-channel electrode array was implanted in a suprachoroidal pocket. Device stability, efficacy, and adverse events were investigated at 12-week intervals.

Results: All four subjects were implanted successfully and there were no device-related serious adverse events. Color fundus photography indicated a mild postoperative subretinal hemorrhage in two recipients, which cleared spontaneously within 2 weeks. Optical coherence tomography confirmed device stability and position under the macula. Screen-based localization accuracy was significantly better for all subjects with device on versus device off. Two subjects were significantly better with the device on in a motion discrimination task at 7, 15, and 30°/s and in a spatial discrimination task at 0.033 cycles per degree. All subjects were more accurate with the device on than device off at walking toward a target on a modified door task, localizing and touching tabletop objects, and detecting obstacles in an obstacle avoidance task. A positive effect of the implant on subjects' daily lives was confirmed by an orientation and mobility assessor and subject self-report.

Conclusions: These interim study data demonstrate that the suprachoroidal prosthesis is safe and provides significant improvements in functional vision, activities of daily living, and observer-rated quality of life.

Translational Relevance: A suprachoroidal prosthesis can provide clinically useful artificial vision while maintaining a safe surgical profile.

Introduction

Retinitis pigmentosa (RP) is the predominant cause of inherited blindness and affects around 2.5 million people worldwide.¹ It is characterized by the progressive loss of outer retinal neurons (photoreceptors) and manifests as a loss of peripheral vision followed by late-stage loss of central vision. Although some progress is being made for selected types of RP with pharmacologic therapies, stem cell transplants, and gene therapies,^{1,2} there is presently no such treatment for the majority of RP subtypes. For individuals with profound vision loss, visual prostheses remain the most viable treatment to improve their functional vision.

A range of technologies exist but, with more than 500 recipients to date, retinal prostheses are the most common type.³ These devices typically incorporate an implantable neurostimulator and an intraocular electrode array, the latter of which can be positioned in epiretinal,⁴ subretinal,⁵⁻⁷ suprachoroidal,^{8,9} and intrascleral¹⁰ locations. In response to processed images from an external image sensor, retinal prostheses can stimulate residual elements of the visual pathway (e.g., bipolar and ganglion cells) to provide rudimentary vision to profoundly blind recipients.

We have previously conducted a phase I clinical trial (Clinicaltrials.gov NCT01603576) using a prototype suprachoroidal retinal prosthesis in three subjects with end-stage RP, and demonstrated that the surgical procedure was feasible, safe, and efficacious, with all subjects showing improvement on localization tasks when compared with device off.⁸ The suprachoroidal surgical approach is attractive owing to decreased surgical complexity and, therefore, a lesser risk of intraoperative and postoperative complications.

Whereas our previous prototype study used a percutaneous connector and was restricted to laboratory-only use, our second-generation device includes implantable stimulators and is suitable for at-home use. The purpose of the present clinical trial is therefore to assess the safety and efficacy of the Bionic Vision Technologies Generation 2 device in subjects with profound visual loss from end-stage RP. The aim of this report was to present the interim results from the first 56 weeks after device switch on.

Methods

Subjects and Eligibility Criteria

Four subjects with advanced retinal dystrophy owing to RP were enrolled in a 2-year study as part of a phase II trial (Clinicaltrials.gov NCT03406416) after

approval from the Royal Victorian Eye and Ear Hospital Human Research Ethics committee (16/1266H). The study was conducted according to the tenets of the Declaration of Helsinki. Written informed consent was obtained from all subjects after explanation of the nature and possible consequences of the study. Both audio and electronic versions of consent information were provided for subject consideration. Eligibility for enrolment included a confirmed diagnosis of RP, a history of at least 10 years of useful form vision, and a functional inner retina (demonstrated by presence of residual bare light perception vision in both eyes). Key exclusion criteria included diseases of the inner retina (including end-stage diabetic retinopathy, retinal trauma, and retinal detachment), optic nerve disease, and any comorbidity that would prevent the clinical team from regularly obtaining ocular images (e.g., dense cataracts or severe and persistent nystagmus). The full list of inclusion and exclusion criteria are shown in Supplementary Table S1.

Potential candidates were screened for eligibility at the Centre for Eye Research Australia. Screening procedures included confirmation of diagnosis, measures of residual visual performance, biometry measures relevant to surgery, psychosocial factors, and willingness to be involved in the study. Visual acuity was assessed using the Berkeley Rudimentary Vision Test and monocular light perception was confirmed using a penlight held close to the eye and Ganzfeld light presentation. Objective refraction was obtained with a handheld autorefractor (ARK-30, Nidek Co., Tokyo, Japan) and axial length was determined with a Zeiss IOLMaster (software V3.02; Carl Zeiss Meditec AG, Jena, Germany). Visual fields were assessed using Goldmann perimetry with target sizes III and V4e. The intraocular pressure was assessed using the iCare TAO1i rebound tonometer (Helsinki, Finland). Full-field electroretinograms (ffERG; Espion, Diagnosys LLC, Lowell, MA) were obtained using DTL electrodes and in accordance with International Society for Clinical Electrophysiology of Vision standards.^{11,12} The full-field stimulus light threshold was determined by asking the subject to verbally respond when they were first able to detect a flash of light as the intensity increased. The diagnosis of RP was confirmed by our lead vitreoretinal surgeon (PJA) after considering each subject's clinical history in conjunction with a dilated ocular fundus examination.

Bionic Vision Technologies Suprachoroidal Retinal Prosthesis (Gen 2)

Generation 2 of the Bionic Vision Technologies suprachoroidal retinal prosthesis contains 44 platinum disc electrodes, each of 1 mm exposed diameter,



Figure 1. (A) The implanted ocular electrode array (left eye variant) shown with two implantable stimulators (image courtesy of D.A.X. Nayagam). (B) External components including a spectacle-mounted CMOS video camera, head-worn magnetically coupled transmission coils, and a body-worn portable video processor (image courtesy of W.G. Kentler).

arranged in a staggered-grid in the leading foveal segment of a 19×8 mm silicone substrate (Fig. 1A). These active electrodes cover 10.00×7.5 mm of retina, corresponding with approximately $37.6 \times 27.6^\circ$ of visual field dependent on lateralization to the fovea.¹³ Two large 2-mm diameter return electrodes are proximal to the temporal edge, and a leadwire of 46 helically coiled insulated platinum wires exits at the superior temporal corner of the substrate. An episcleral silicone patch is incorporated in the lead to cover the sclera exit point and provide mechanical fixation for the cable as it leaves the eye. Similarly, the lead incorporates a silicone grommet for fixation of the cable onto the zygomatic bone as it exits the eye orbit. The device was manufactured in both left and right eye variants.

Electrical stimulation of the electrodes is achieved by two current sources, packaged in two separate hermetically sealed titanium stimulator packages implanted under the postauricular scalp (Fig. 1A). Each stimulator addresses 22 independent electrodes. Phosphene persistence for camera use was optimized with 500-ms rest periods interleaved throughout the stimulation sequence. Power and data transfer occur via head-worn magnetically coupled transmission coils. The visual scene is continuously captured by a CMOS video camera mounted on the arm of a pair of secure-fitting, custom-molded spectacles and processed into suitable signals for the implanted stimulators by a body-worn portable video processor (Fig. 1B). Images are filtered by the processor using a Lanczos2 filter to improve edge detection and contrast.¹⁴ During mobility assessments (modified door task and obstacle avoidance, described elsewhere in this article) images were always inverted such that the strongest stimulation corresponded with the darkest spots in the image. During home use, subjects were able to select between

noninverted and inverted modes using buttons on the video processing unit (Fig. 1B).

Implantation Surgery

Eligible subjects had the device implanted by experienced vitreoretinal surgeons (PJA and JY) in collaboration with an otolaryngologist (RB) at the Royal Victorian Eye and Ear Hospital between February and August 2018. The surgical procedure followed the methods previously refined and described.^{8,15} General anesthesia was administered and a dummy implant with a leadwire was used for surgical planning and marking of the scalp. A C-shaped incision was made following the curve of the scalp posterior to the pinna to expose a flat section of squamous temporal bone for placement of the stimulator packages. A tunnel was then created beneath the temporalis fascia and muscle forward to the lateral orbital rim.

A lateral canthotomy was performed, then the orbital margin of the eye socket was exposed and a lateral orbitotomy was created to provide a notch for stabilizing the grommet. At this stage, the intraocular electrode array and leadwire were loaded into a custom trocar and passed forward from the postauricular incision, under the fascia and muscle, to the lateral canthotomy/lateral orbital margin.

A temporal peritomy was performed to expose the sclera and lateral rectus muscle before the lateral rectus muscle was disinserted. A scleral wound was made and the suprachoroidal space was dissected with a crescent blade and a lens glide.

The electrode array was inserted with forceps into the dissected suprachoroidal pocket and the position and integrity of the device were checked with fundus examination and electrical impedance testing,

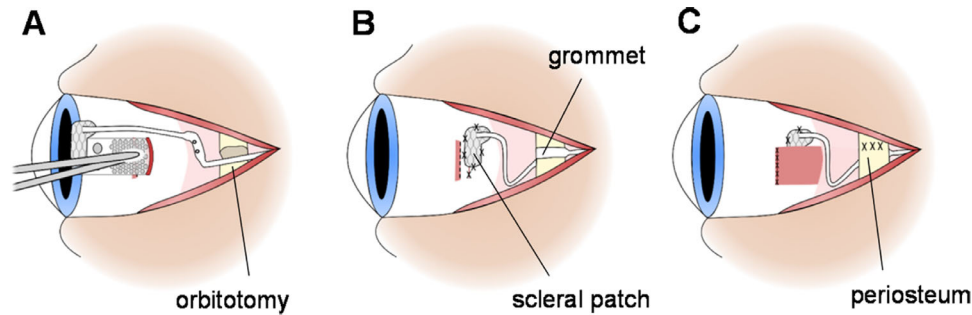


Figure 2. Indicative ocular aspects of the surgical procedure: (A) The electrode array is inserted into the dissected suprachoroidal pocket. (B) The Dacron patch is sutured to the eye globe and the lead grommet is placed within the orbitotomy. (C) The lateral rectus muscle is replaced and the periosteum is closed over the lead.



Figure 3. Study flowchart. All time points are relative to device switch-on and basic fitting in week 1. Weeks 2 to 16 included training on camera use, head scanning, mobility, and task familiarization. Functional assessments comparing device on versus device off occurred in week 17, with repeated assessments at week 20, 32, 44, and 56.

respectively. The scleral wound was closed and a Dacron patch was sutured to the sclera over the wound to stabilize the lead-wire exit and protect the wound site (Fig. 2). The lateral rectus muscle was then reattached.

With the ocular procedures completed, the lead-wire was fixated in the orbitotomy by a silicone grommet and the periosteum closed over. The post auricular skin incision was repaired. A sub-Tenon local anesthetic block was given for short-term pain relief before a pressure dressing was applied to the surgical site.

Subjects remained in the hospital for 4 to 5 days of postoperative care before being discharged. Intravenous antibiotics were administered for 48 hours, followed by oral antibiotics for 5 days. Topical broad-spectrum antibiotics, steroids, and oral analgesia were administered as required. During this period, impedance testing of the implants was performed daily. After discharge, eye examinations were performed weekly with a slit lamp, indirect ophthalmoscope, and optical coherence tomography (OCT) to assess corneal clarity, vitreous inflammation, and fundal appearance. The external lateral canthotomy and postauricular wounds were monitored at each postoperative visit for signs of healing and/or infection.

At 7 to 9 weeks after surgery (Fig. 3), subjects commenced fitting (week 1) and training (weeks 2–16) with the device. All stated time points are relative to device switch-on (week 1).

Clinical Outcomes

The primary study outcome measure was the number and severity of device related serious adverse events (SAEs) during the period of 2 years after the surgery. In this interim report, we are reporting device stability and functional vision data up to week 56 (approximately 1 year) after device switch on, which is 63 to 65 weeks after surgery. Seven secondary outcome measures related to visual function and functional vision were measured at week 17 and week 20 after switch on and every 12 weeks thereafter. Visual response thresholds were measured using a two-down one-up modified staircase procedure.¹⁶ This study complied with the Recommendations of the Task Force for the Harmonization of Outcomes and Vision Endpoints in Vision Restoration Trials.¹⁷

Screen-based Assessments

Localization ability, motion discrimination, and spatial discrimination were assessed in a visual-function test battery using high-contrast optotypes presented on a 40-inch touchscreen at the subject's arm's length (Fig. 4A). To assess retinotopic discrimination,^{17–19} a scrambled condition with nonretinotopic mapping between points in the visual field and specific electrodes (re-randomized every 5 seconds to avoid familiarization) was included in the localization and

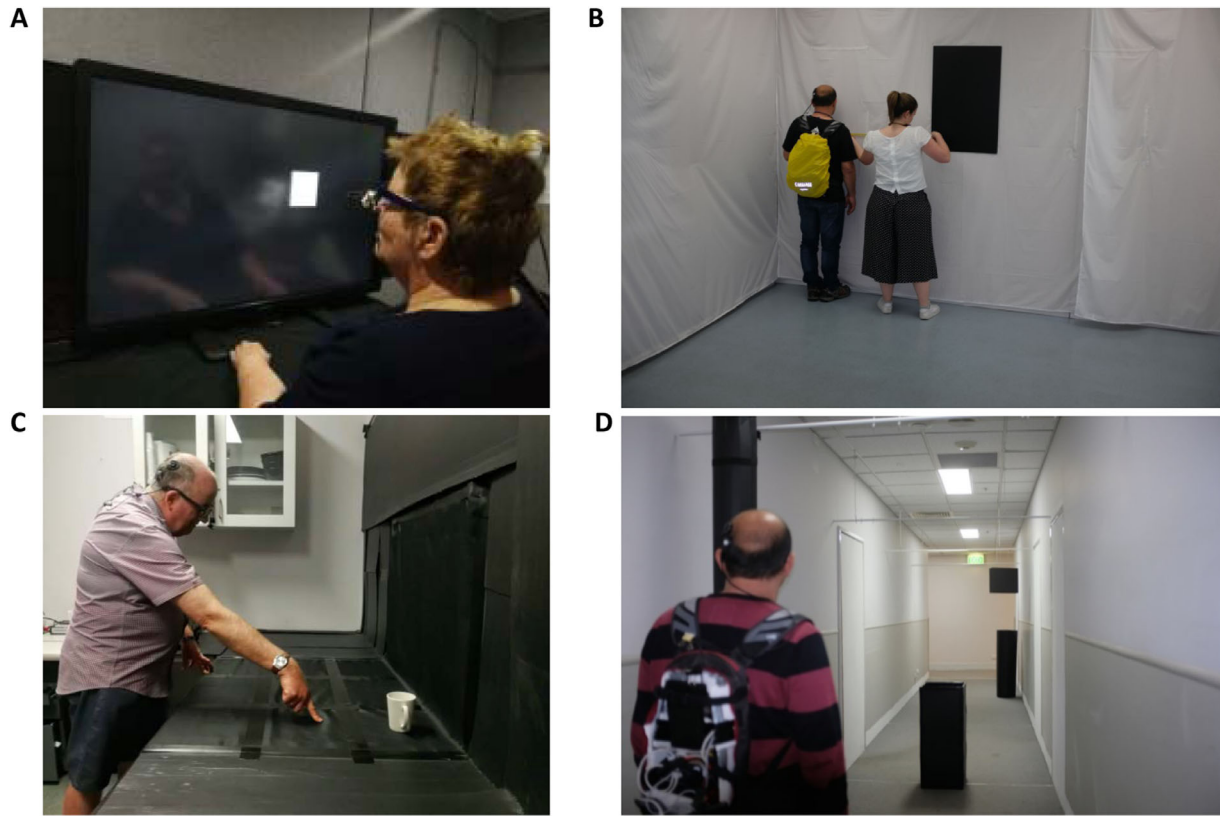


Figure 4. (A) Screen-based tasks were performed on a 40-inch touchscreen at arm's length. Shown here is the square localization task. (B) Measuring fingertip distance to target in the modified door task. (C) Tabletop search task. (D) Obstacle avoidance task. The subjects are shown in (B) and (D) wearing a backpack containing wireless equipment for remote control of device parameters.

motion discrimination tasks. Scrambling the electrode mapping allows objective comparison with normal mapping, with impaired performance highlighting a subject's perceptual access to retinotopic information in normal operation.^{17–19} Subjects were masked to the test condition and were unaware of the existence of the scrambled condition, but became quickly aware when the device was in the off condition. Viewing distance was measured before each task and stimulus sizes were adjusted by the test program accordingly. For a typical viewing distance of 43 cm, the 40-inch monitor spanned $95 \times 63^\circ$ of visual arc. Subjects had their nonimplanted eye patched during all screen-based tasks and were free to move their heads.

For localization, the subject was instructed to locate and accurately touch the center of 10° wide squares that appeared in random locations. Performance (pointing error) was quantified for each trial as the distance (vector magnitude) between the target center and the point touched, including cases where the pointing location was within the target boundaries. The average error for each condition was calculated as the average of distances without consideration of the direc-

tion of the error. There were 24 trials total per condition (device on, device off, and scrambled) with a block size of eight trials per condition in a balanced randomized design. If a trial exceeded 30 seconds, a repetitive alarm compelled a prompt response.

For motion discrimination, a single 5° wide bar moved perpendicularly across the screen in one of four cardinal directions, and the subject indicated direction of movement using a keypad (four-alternative forced choice, 24 trials total per condition, block size of 8 trials per condition with balanced representation of stimulus direction). This task was repeated at up to three speeds, namely, 7, 15, and $30^\circ/s$, with subjects progressing to the next speed if their score significantly exceeded chance (25%). All trials were completed within 30 seconds.

Spatial discrimination was assessed from week 32 using the Basic Grating Acuity test program.²⁰ The screen was evenly divided into horizontal or vertical black and white stripes (2-alternative forced choice, 24 trials per condition). Spatial discrimination was first assessed at 0.033 cycles per degree (cpd) and then repeated at a higher spatial frequency (0.1 cpd), if

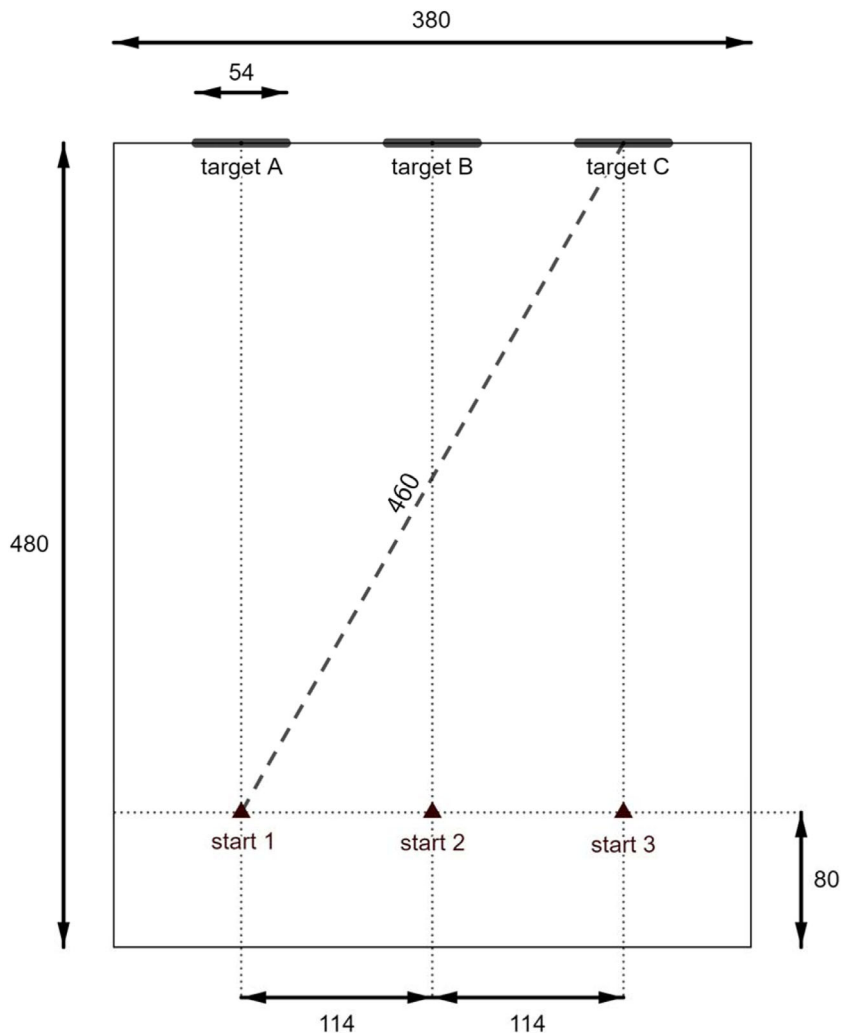


Figure 5. Configuration of the modified door task. All measurements are in centimeters. A black high-contrast target, representing a darkened window or doorway, was randomly positioned at location A, B, or C. The target measured 54 × 70 cm (W × H) and the top-edge was approximately 2 meters above the floor. Subjects started each trial at a random selection of starting points 1, 2, or 3.

the participant exceeded the passing criterion (75% accuracy), or at a lower spatial frequency (0.01 cpd), if they did not. Trials exceeding 30 seconds were automatically scored as incorrect by the test program.

Modified Door Task

This task, modelled on a previously described door task, which used a larger target,²¹ determined whether subjects could detect, walk toward, and touch a high-contrast (i.e., black) target (54 × 70 cm) in a white-walled room measuring 3.8 × 4.8 m (Fig. 4B). The start position (1, 2, 3) of the subject along the baseline and the target location (A, B, C) on the finishing wall were separately randomized (10 trials per condition) (Fig. 5). The required traversal distance varied between 4.0 and 4.6 m, depending on the start and end positions. When

the subject was satisfied they were within reach of the target, they announced stop and reached for the target. Measurements included distance from finger tip to the nearest edge of the target and time to complete each trial. Successful touches were ascribed a distance of zero.

Tabletop Search

One of six common household objects (plate, bowl, placemat, cup, can, or fork) was randomly selected and placed at one of nine locations of a 3 × 3 grid measuring 109 × 81 cm total (each grid cell measuring 36 × 27 cm). This task has been validated previously to stratify subjects with low vision according to visual acuity and remaining visual field.²² All objects (except the silver fork) were colored white, in contrast

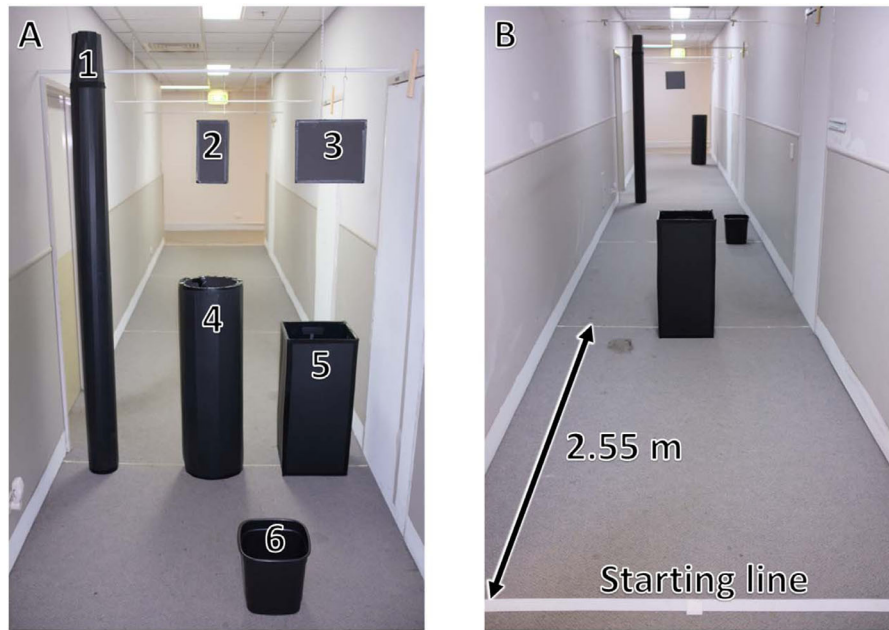


Figure 6. (A) The six obstacles used to seed the obstacle course: (1) tall pole (17 × 230 × 17 cm); (2) small box – hanging (15 × 30 × 10 cm); (3) large box – hanging (33 × 30 × 10 cm); (4) short pole (34 × 107 × 34 cm); (5) large wastepaper basket (34 × 78 × 34 cm); (6) small wastepaper basket (28 × 34 × 28 cm). (B) An example configuration of the obstacle course. A random selection of five of the six obstacles were placed at 2.55-metre intervals along a 1.75 × 20.00 m corridor.

with the black tabletop surface (Fig. 4C). Room illumination was maintained around 300 ± 40 lux. From a standing position, subjects were told to first verbalize the object location, attempt to identify, and then reach for the object with their fingertip. There were 20 trials per condition (device on vs. device off) in a randomized order. Selection of object and location from the pool of 54 potential combinations was randomized by computer (www.random.org) without balancing.

Subjects were reminded of the object selection at the start of each session and encouraged to touch and view the objects using their prostheses before the task commencing. Outcome measures included accuracy of verbalized location, response time, object identification, successful contact with the object, and distance from fingertip to nearest edge of the object. Successful touches were ascribed a distance of zero.

Obstacle Avoidance

Subjects were assessed on their ability to detect and avoid five obstacles while walking down a 20-m corridor (1.75 m wide) without their usual mobility aid for 10 trials with device on and 10 trials with device off in randomized order (Fig. 4D). Each trial was seeded with a random selection of five of six possible obstacles (tall and short poles, small and large wastepaper baskets, and small and large hanging boxes at head

height) placed at 2.55-m intervals along the corridor at one of three locations (center, left of center, or right of center, Fig. 6). Each obstacle location was represented five times per three trials. Preferred walking speed with a sighted guide was assessed for two obstacle-free traversals of the corridor before task commencement. Outcome measures included verbal indication of objects detected, frequency of obstacle contact, task completion time (as a percentage of the preferred walking speed), and percentage of trials with zero collisions or contact. As subjects might find some obstacles more difficult to detect or avoid than others, we also calculated the overall detection rate and contact rate for each obstacle type and location.

Functional Low Vision Observer Rated Assessment (FLORA)

The FLORA instrument (Second Sight Medical Products, Sylmar, CA)²³ was used to evaluate presurgery functional vision and mobility, and provide comparisons between device on versus device off at postsurgery outcome measure time points. The FLORA instrument comprises a series of questions relating to daily living experiences (e.g., self-assessment of if/how the device has improved their life) and a selection of functional vision tasks that are graded

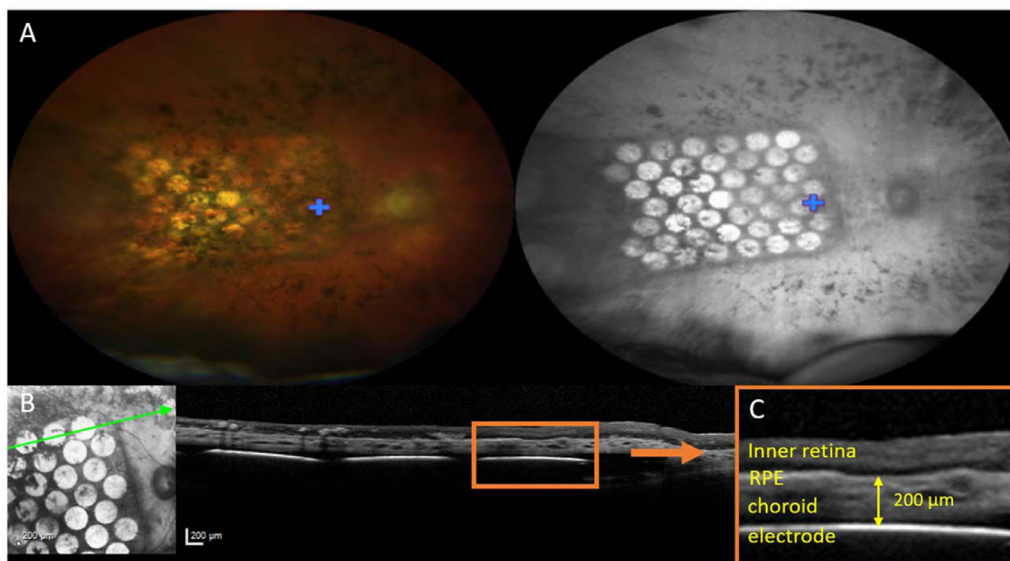


Figure 7. (A) Fundus images of the electrode array at 12 weeks after surgery for a right eye implantation (S4), visualized using a CLARUS 500 in wide-field configuration (133° retinal field) with RGB illumination (*left image*) and infrared illumination (*right image*). A blue cross marks the fovea. The leading edge of the electrode array is surgically inserted toward the optic disc, with the trailing edge and lead wire (not shown) extending toward the periphery. (B) OCT image of the electrode array at 4 weeks after surgery (S2). (*Left*) The infrared image was used to orientate the B-scan position (*green line*) through the retina and electrode array. (*Right*) The retina and electrodes could be visualized on OCT B-scan. (C) Magnified view of the region in the orange box in (B), showing the inner retina, RPE, choroid, and suprachoroidal electrode. The yellow arrow demonstrates an example measurement of electrode-to-retina distance (200 µm), defined as the distance from electrode to the outer retina boundary.

by an orientation and mobility specialist (e.g., the ability to determine the direction of travel of a person walking). These evaluations were conducted at the subject's residence and habitual environments such as workplace and were restricted to tasks identified as being relevant to each subject's self-reported goals and activities. Each completed task was graded as being easy to impossible and graphed as the mean subject score across four categories: orientation, mobility, activities of daily living, and interacting with others. In addition, the contribution of vision to task completion (as opposed to other senses) was assessed for these same categories.

The overall impact of the retinal prosthesis on daily life was deduced by an independent examiner from both the self-report and functional vision components of the FLORA. A positive outcome was recorded when the subject self-reported an improvement in well-being and/or functional vision and the orientation and mobility assessor observed the improvement. A neutral outcome was recorded when the subject and the assessor felt the device had not made a positive or negative impact. A negative outcome was recorded when the subject indicated that the device had worsened their life in some aspect.

Quality-of-Life Assessments

Vision-related quality-of-life was quantified using the Impact of Vision Impairment – Very Low Vision (IVI-VLV)²⁴ questionnaire, which includes two subscales: activities of daily living, mobility, and safety (16 items) and emotional well-being (12 items). The presence and degree of depressive effect was monitored using the Patient Health Questionnaire-9²⁵ to allow differentiation of the impacts of depression on the other quality-of-life outcome measures.

Device Stability

In addition to ongoing assessments of ocular health, color retinal photography (fundus) and OCT were obtained throughout the study (Fig. 7). Any relative changes to position of the array laterally or axially over time were observed.

Color fundus photographs of the macula and optic nerve head were acquired using a Topcon Medical Systems TRC-50EX (Tokyo, Japan) retinal camera and at some visits additionally with the Clarus 500 (Carl Zeiss Meditec AG) widefield retinal camera. Subjects were dilated with topical 0.5% tropicamide

and additional 2.5% phenylephrine if required for adequate pupil dilation.

OCT B-scans were acquired using a Spectralis OCT (Heidelberg Engineering GmbH, Heidelberg, Germany). Infrared imaging was used to orientate the single section line scan either horizontally or vertically through the retina and electrode array. For electrodes that could be reliably visualized, electrode-to-retina distances were measured in microns from the center of the electrode to the inner boundary of the retinal pigment epithelium (Fig. 7C), using the manufacturer-provided Heyex software (version 1.10.20.0).

Statistical Analyses

Performance with device on was compared with device off and, for the localization and motion discrimination tasks, with the scrambled condition. Statistical significance across conditions at the subject level was assessed in R version 3.6.3 (R Foundation for Statistical Computing, Vienna, Austria) using the nonparametric Friedman test,^{26–28} which allows for differences across multiple test dates. Post hoc comparisons were performed with Conover's nonparametric equivalent of Fisher's least significance difference method.²⁹ In a few cases, an outcome measure was missed owing to participant absence, timing constraints, or fatigue, or block sizes were unequal owing to procedural error. In these instances Wittkowski's variant of the Friedman test (which is tolerant of incomplete blocking) was used for within-subject comparisons.^{26,28}

Performance in the spatial discrimination task was considered significantly above chance if accuracy was greater than 75% (i.e., $P < 0.05$ for a binomial distribution of 24 trials). Because the tasks were repeated at multiple time points, linear regression analyses were run to assess whether subjects' performance changed over the course of the study. Family-wise errors within each task were controlled using Holm's sequential correction.³⁰

Results

Four subjects, aged 39 to 66 years, were enrolled and successfully implanted with the suprachoroidal implant unilaterally (Table). The surgical procedures took between 204 and 260 minutes and were uncomplicated. At the completion of surgery, impedance testing showed that all electrodes were functional in all subjects. At 56 weeks after switch on, 97% of all electrodes were functional (decrease of 0–3 electrodes per subject). The remaining electrodes were intermittently high impedance, suggesting ductile stretching in the affected lead-wires. There have been no serious or unexpected adverse events relating to the surgery or device for the study to date (64 weeks after surgery).

Clinical Outcomes

There were no device-related SAEs in this trial.

Clinical examination of all four eyes showed routine postoperative recovery with a small trace of

Table. Subject Demographics

Feature	S1	S2	S3	S4
Gender	Male	Male	Female	Male
Age at implant (years)	47	63	66	39
Eye condition	RP (rod cone)	RP (rod cone)	RP (cone rod dystrophy)	RP (cone rod dystrophy, diagnosis as an infant)
Observed nystagmus	Mild	Intermittent	None	Mild
Visual acuity	Light perception OU	Light perception OU	Light perception OU	Light perception OU
ffERG stimulus light threshold (candela s/m ²)	0.1	0.1	0.001	0.001
Age when legally blind	20	34	41	13
Approximate years of useful form vision	34	43	56	19
Primary mobility aid	Cane	Cane	Guide Dog	Cane
Implanted eye	Left	Right	Right	Right

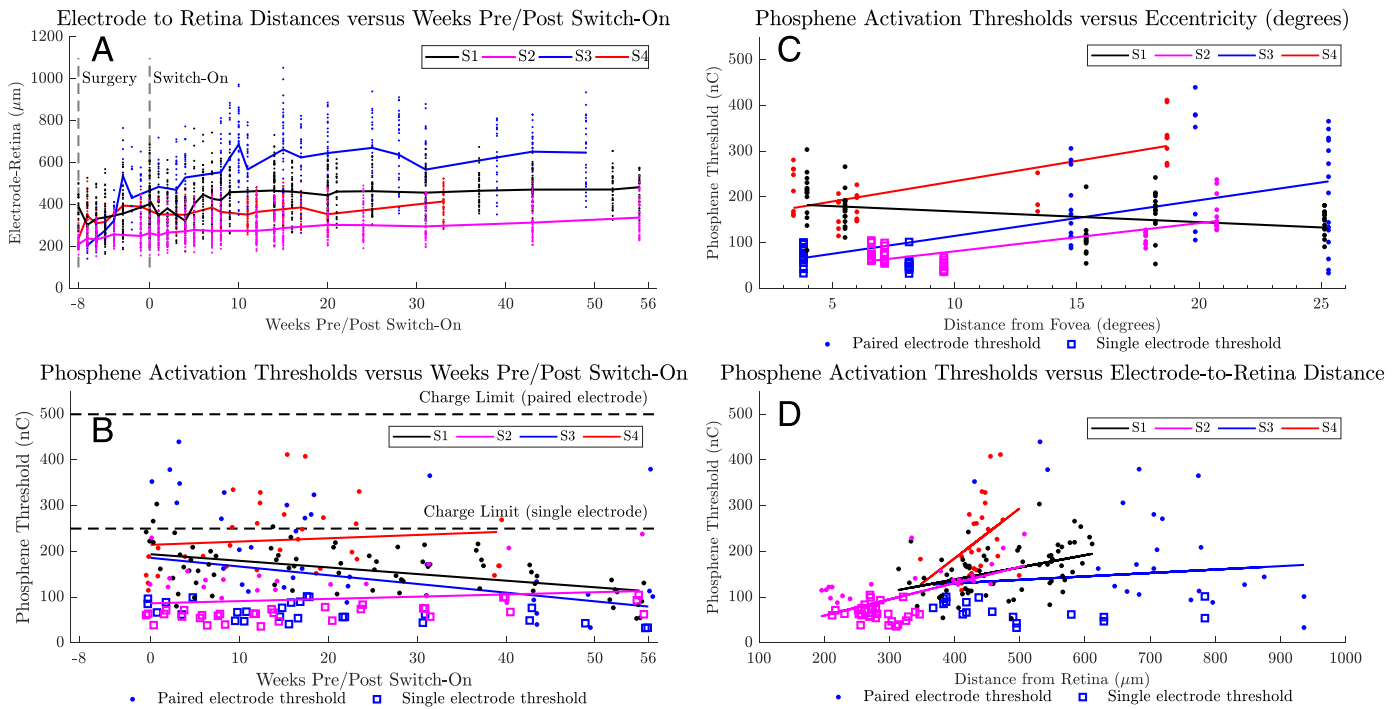


Figure 8. (A) Electrode to retina distances obtained from OCT images. Each different color (*black, magenta, blue, red*) indicates data for each subject. Individual electrode measurements are shown as dots. A solid line connects the median values between time points. A vertical line at -8 weeks indicates the date of surgery. A vertical line at 0 weeks indicates the date of device activation ('switch-on'). (B) Device thresholds for a subset of five phosphenes per subject were assessed throughout the 56-week period. Phosphenes are typically in a single electrode configuration (*open squares*) for electrodes nearest the fovea and paired electrode configuration (*solid dots*) for electrodes at the periphery where higher charge requirements have been observed. Defined safe charge limits of 250 nC (single electrode) and 500 nC (paired electrode) are indicated with dotted horizontal lines. A *solid line* describes a linear regression for each subject. (C) Device thresholds for the same subset of five phosphenes per subject versus eccentricity from the fovea (degrees). A *SOLID LINE* describes a linear regression for each subject. (D) Device thresholds for the same subset of five phosphenes per subject versus electrode-to-retina distance (in micrometers). A *solid line* describes a linear regression for each subject.

subretinal hemorrhage in two recipients. The first of these was approximately 1 optic disc diameter at its broadest and extended from the leading edge along the inferior margin of the device. The second hemorrhage was 2×2 disc diameters in the inferonasal portion of the array. Both hemorrhages presented as only mild obscuration of the electrodes on color fundus photograph, and cleared spontaneously within 2 weeks.

The remainder of adverse events related to surgery were all expected events: pain around the stimulator region, swollen eyelid, tenderness of the operated eye and lateral canthus, conjunctival injection, ocular pressure sensation, and minor inflammation of the anterior chamber. One subject experienced an increased intraocular pressure in response to the topical steroids used for eyelid oedema. The pressure decreased with a decrease in the steroid dose and administration of topical intraocular pressure-lowering medication for 11 days. Fundus and OCT imaging confirmed the device position under the macula and the absence of retinal trauma (Fig. 7).

Device Stability and Safety

The electrode-to-retina distances seem to have been increasing over time (Fig. 8A), with the greatest rate of increase being in the period immediately after surgery (weeks -8 to 0). Short-term bias may be attributed to difficulty in visualizing a complete set of electrodes. By week 20, the rate of increase has slowed for all subjects.

In one subject (S1, black line, Fig. 8A) the implant and retina were displaced anteriorly during weeks 2 to 4 (i.e., 10–12 weeks postoperatively), resulting in a 6-diopter increase in the OCT focus. Fundus imaging showed no evidence of hemorrhage and the displacement, potentially owing to a choroidal effusion, spontaneously settled by week 8 without intervention.

Analyses of visualized position of the leading edge of the implant suggested some minimal rotation (maximum 17° across subjects) and translation temporally (maximum $252 \mu\text{m}$ across subjects) in the first 25 weeks, which subsequently settled and remained stable (Allen PJ, et al. IOVS 2020;61:ARVO E-Abstract 2200).

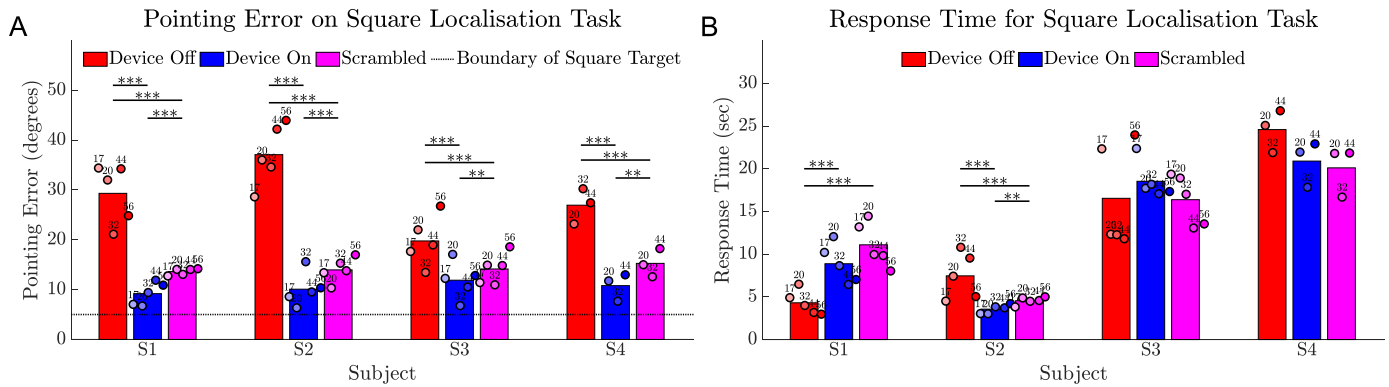


Figure 9. Results for the square localization task comparing device on (blue) versus device off (red) versus a scrambled condition (magenta). **(A)** Average pointing error (in degrees) from touch location to the target center for 24 trials of each condition. The boundary of the 10° wide square target is indicated by a dotted horizontal line. **(B)** Average response time (seconds) for 24 trials of each condition. Circles show the average of 24 trials at each time point, shaded progressively darker for later dates and labelled with week number. The height of the bar is each subject's average across all time points. Statistical significance of within-subject comparisons is shown; *** $P < 0.001$, ** $P < 0.01$.

These small shifts did not necessitate any change to camera image sampling locations.

Device Thresholds

The average phosphene thresholds in the first 4 weeks after switch on were 182 ± 96 nC, (range, 38–454 nC). Subjects described phosphenes near the fovea as having defined shapes (e.g., “like a circle the size of a 5 cent piece”), whereas phosphenes at the periphery were described as having less definition (e.g., “like a light being turned on at the end of a long corridor”). Subjects did not report short-term or long-term fading, although faint spontaneous visual activity was reported after days with above average device use.

Figure 8B details the thresholds for a subset of five phosphenes per subject, chosen to include a selection of foveal or parafoveal phosphenes and the most eccentric phosphenes per subject, tracked regularly around outcome measures and clinic visits. Electrodes at the periphery were used in a paired configuration to maintain safe charge limits, defined from our preclinical studies as 250 nC for a single electrode and 500 nC for a pair (Nayagam DAX, et al. IOVS 2017;58:ARVO E-Abstract 4204). Although electrode combinations were not tested exhaustively, the phosphene yield obtained within safe limits was 27 of 44 electrodes (61.4%) for S1, 32 (72.7%) for S2, 24 (54.5%) for S3, and 25 (56.8%) for S4, comprising predominantly foveal electrodes with sparser density at the periphery.

Despite the observed increases in the electrode-to-retina distances (Fig. 8A), thresholds for subjects S1 and S3 seemed to decrease over time, suggestive of phosphene familiarization. For the remaining two subjects, the fitted regression line for subject S2

increased by 27 nC between weeks 0 and 56 and for subject S4 increased by 28 nC between weeks 0 and 39.

Figure 8C details the relationship between threshold and eccentricity for the subset of phosphenes presented in Figure 8B. Activation thresholds appeared positively correlated with phosphene eccentricity for subjects S2 to S4, with gradients between 6.16 to 8.88 nC/degree (all $P < 0.001$). Subject S1 had a negative correlation of -2.33 nC/degree ($P < 0.01$). This result was not unexpected because, in contrast with the other three subjects, the electrode-to-retina distances for subject S1 were greatest at the fovea.

Figure 8D details the relationship between threshold and OCT electrode-to-retina distance for the subset of phosphenes presented in Figure 8B. Activation thresholds were positively correlated with electrode-to-retina distance for S1 (0.27 nC/ μm , $P < 0.001$), S2 (0.36 nC/ μm , $P < 0.001$), and S4 (1.09 nC/ μm , $P < 0.05$). The linear regression for S3 was not significant (0.08 nC/ μm , $P = 0.48$).

Screen-based Assessments

Square-Localization Task

The touch accuracy of the 10° square optotype was significantly better with device on than device off for all subjects (all $P < 0.001$) (Fig. 9A). Subject averages for pointing error from target center ranged from 9.2° to 11.9° (device on) versus 19.8° to 37.1° (device off) versus 13.6° to 15.3° (scrambled). Pointing error in the scrambled condition was significantly worse than device on but better than device off for all subjects (all $P < 0.001$, except $P < 0.01$ for S3 and S4, scrambled vs device on). Response times were shortest for subjects S1 and S2 (Fig. 9B).

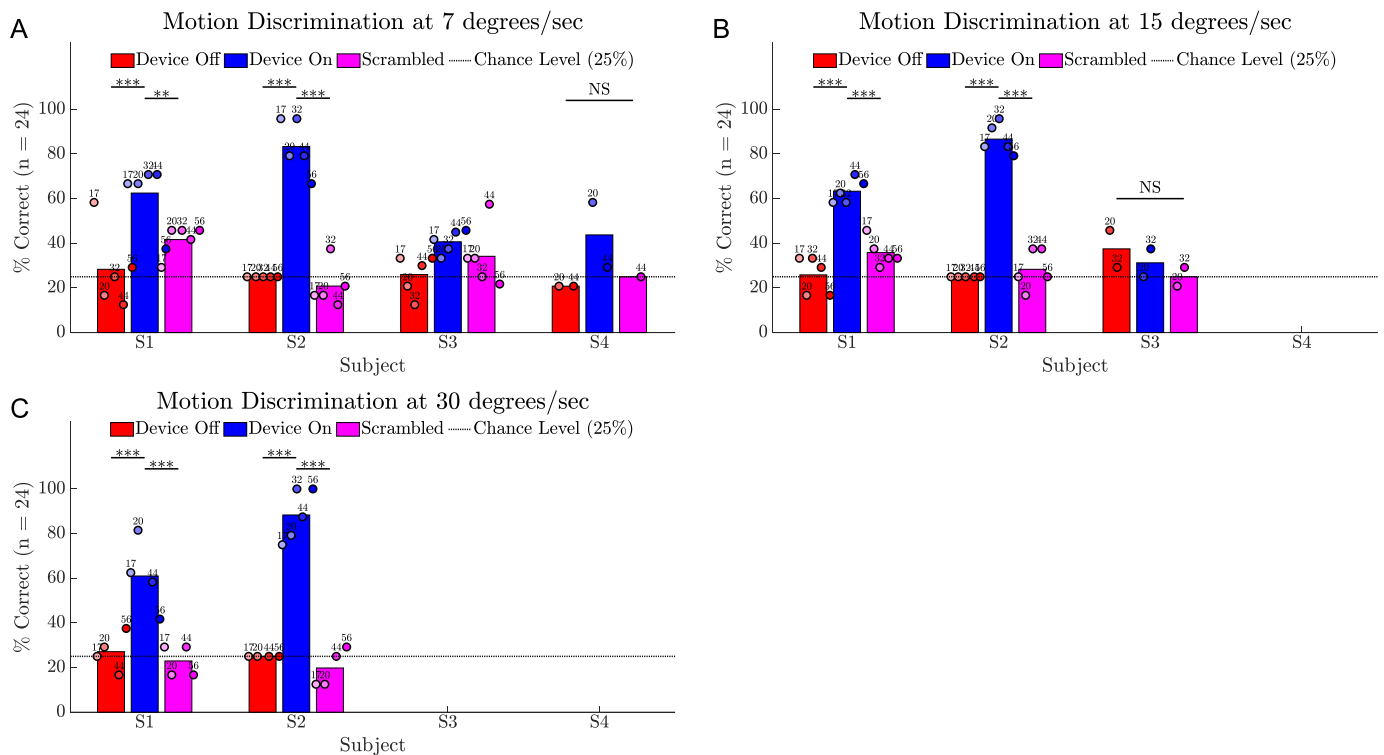


Figure 10. Results for the motion discrimination task comparing device on (blue) versus device off (red) versus a scrambled condition (magenta). (A) Success rate at 7°/s. (B) Success rate at 15°/s. (C) Success rate at 30°/s. Chance level (25%) is shown as a dotted horizontal line. Circles show the average of 24 trials at each time point, shaded progressively darker for later dates and labelled with week number. The height of the bar is each subject's average across all time points. Statistical significance of within-subject comparisons is shown; *** $P < 0.001$; ** $P < 0.01$; NS = not significant. Friedman tests for S3 at 7°/s were significant, but post hoc comparisons were not; hence, significance is not indicated for these data.

Motion Discrimination

All subjects completed the motion discrimination task at 7°/s (Fig. 10A) with subject S1 and S2 averages for success rate being significantly better with device on (62.5% and 83.3%) versus device off (28.3% and 25%; $P < 0.001$). A subset of subjects completed the task at 15 and 30°/s (Fig. 10B-C): subjects S1 and S2 continued to demonstrate a significant benefit of device on ($P < 0.001$), whereas subject S3 scored near chance at 15°/s and did not attempt 30°/s. The success rate with the scrambled condition was significantly poorer than with device on for subjects S1 and S2 (all $P < 0.001$, except $P < 0.01$ for S1 at 7°/s), with the greatest impact on performance observed for subject S2 at 30°/s (19.8% average score with scrambled vs. 88.3% average score with device on). It is notable that subject S1 scored 60% at 7°/s with device off on one occasion (week 17). Although this is unusual statistically, ophthalmological assessments confirmed that he has no useful natural vision in his implanted eye. His device off performance was at chance levels for all subsequent measurements and, as for the other subjects, his

nonimplanted eye was patched for all screen-based assessments.

Linear regressions to examine within-subject changes in performance over the study for the screen-based tasks did not reach significance in any comparisons.

Spatial Discrimination

Subject S4 did not attempt the spatial discrimination task, subject S3 attempted at weeks 44 and 56, and subjects S1 and S2 attempted at weeks 32, 44, and 56. Incomplete data are due to the high levels of fatigue that this task caused the subjects, which limited the usefulness of the measure. Figure 11A demonstrates that the passing criterion of 75% on 24 trials of the two-alternative forced choice basic grating acuity spatial discrimination task with a grating spacing of 0.033 cycles per degree was met or exceeded on one occasion for subject S1 (range, 62.5%–75%) and on three occasions for subject S2 (range, 75%–87.5%; $P < 0.05$). Shorter response times with device off (Fig. 11B), particularly for subject S1, suggest decreased

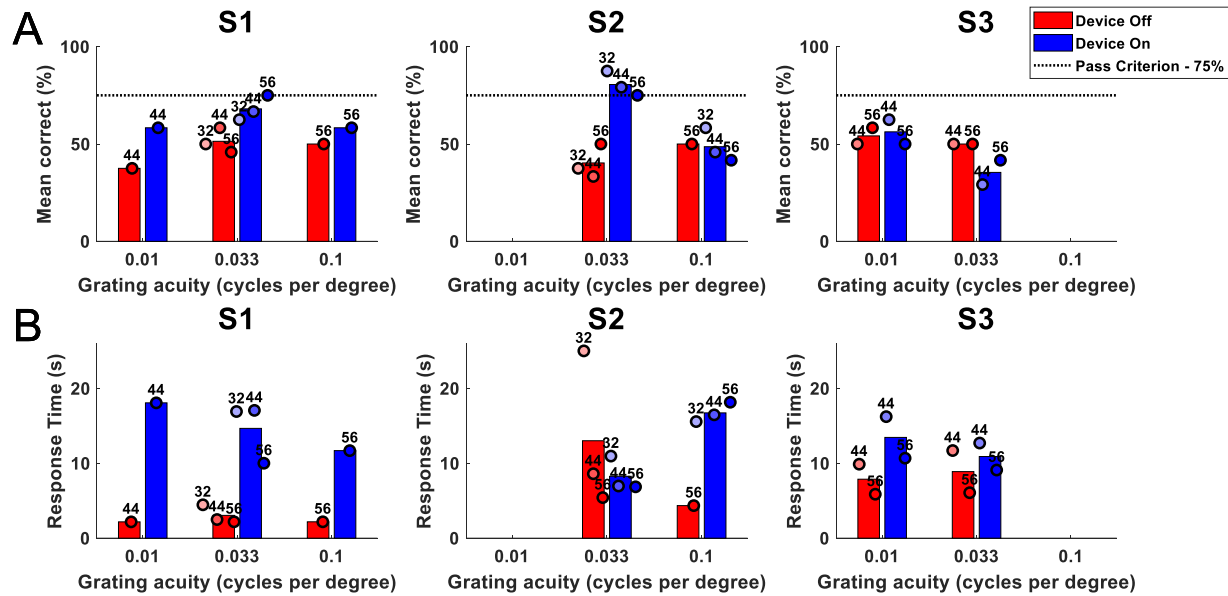


Figure 11. Results for the spatial discrimination task comparing device on (blue) versus device off (red) for subjects S1 to S3. **(A)** Percentage correct of 24 trials. The passing criterion (75%) is shown as a dotted horizontal line. **(B)** Mean response time (seconds). Circles show the average of 24 trials at each time point, shaded progressively darker for later dates and labelled with week number. The height of the bar is each subject's average across all time points. Significance was not tested. Subject S4 did not attempt this task.

task engagement when the camera was disabled. The percentage of trials that exceeded 30 seconds (and were scored as incorrect) was less than 5% for each subject (range, 0.5%–3.4%).

Functional Assessments

Modified Door Task

All subjects could complete the task and subjects S1, S2, and S4 were significantly more successful with device on at reaching and touching the target (Fig. 12A) ($P < 0.001$). Subjects were observed to use the perceived width of the target to determine proximity, describing that the target was visible for a greater visual arc during head scanning when they were close by. Subject averages for distance between fingertip and target ranged from 62.6 to 95.4 cm with the device off and 4.8 to 29.5 cm with the device on (Fig. 12B) and were significantly better than device off in all cases ($P < 0.001$). The time to complete the task was longest for subject S3 (Fig. 12C), commensurate with observed challenges in distance estimation for this subject during the task.

Tabletop Search

All subjects were significantly better at verbally localizing objects with the device on than with the device off (Fig. 13A) ($P < 0.001$ for S1, S2, and S4; $P < 0.01$ for S3). Subject averages for object identifi-

cation scores were significantly higher with device on than with device off for subjects S1 and S2 (both $P < 0.05$), but were less than 40% on average (Fig. 13B).

An improvement in hand–camera coordination was confirmed with significantly higher success at touching the object with device on for subjects S1, S2, and S4 (all $P < 0.001$) (Fig. 13C). Subject averages for distance between fingertip and object were 4.1 to 13.3 cm with the device on and 19.6 to 37.3 cm with the device off (Fig. 13D), and were significantly better with the device on ($P < 0.001$ for S1, S2, and S4; $P < 0.05$ for S3). Subjects S3 and S4 experienced intermittent shoulder pain, unrelated to the device, but a consequence of this was some systematic undershoot when reaching for objects in the back row.

Localization and touch results for subject S3 with the device off were notably better than for other subjects but still poorer than with the device on. Although subject S3 has no measurable islands of vision for either eye on Goldmann perimetry, she reported that she could detect tabletop objects by noticing changes in contrast (“shadows”) as she performed head scanning.

Comparisons with device on for reported object versus actual object (Fig. 14A) demonstrate clustering of responses according to the size of the actual object—visible as the dark band of cells from the lower left to the upper right of the matrix. Confusion with device on seemed to be more likely to be between objects of

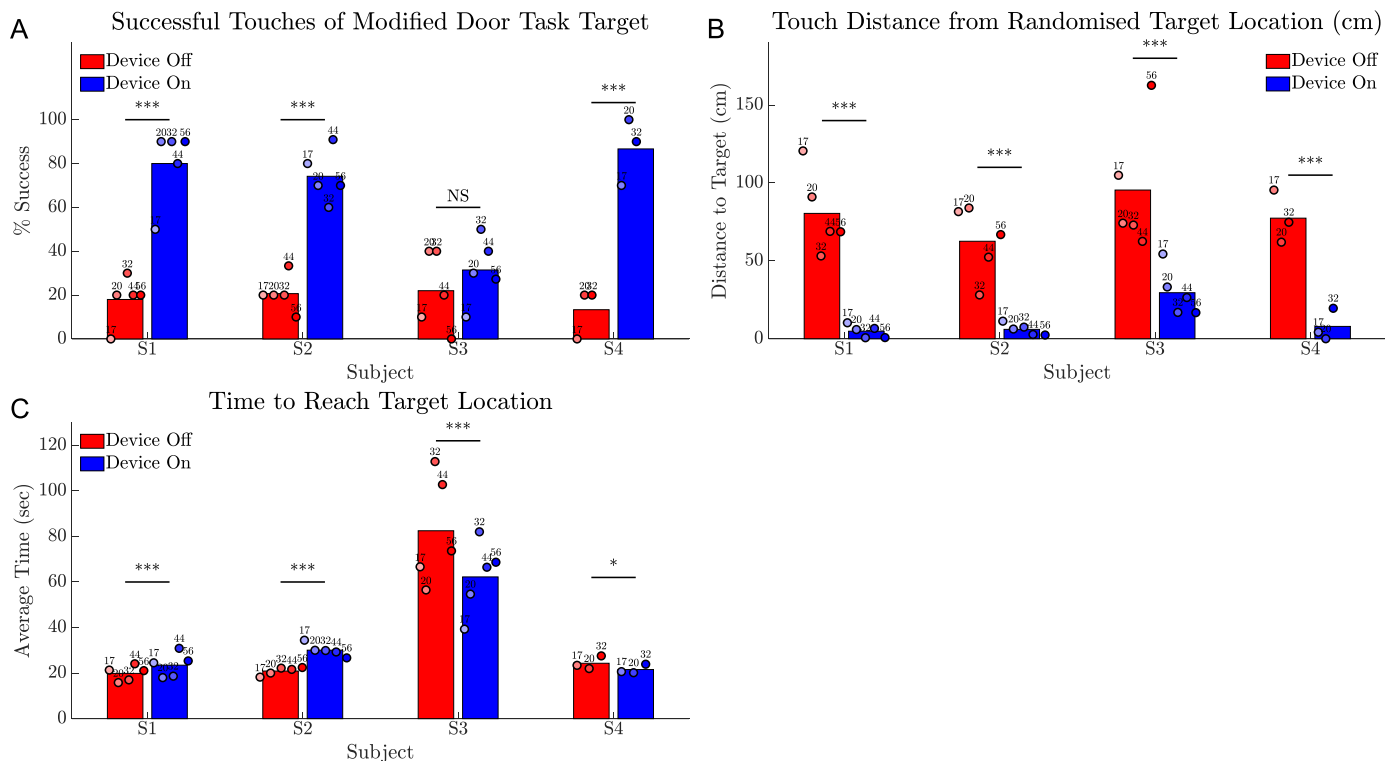


Figure 12. Results for the modified door task comparing device on (blue) versus device off (red). **(A)** Rate of successful touches of target (%). **(B)** Touch distance from fingertip to target including successful touches. **(C)** Time taken to reach target. Circles show the average of 10 trials at each time point, shaded progressively darker for later dates and labelled with week number. The height of the bar is each subject's average across all time points. Statistical significance of within-subject comparisons is shown; *** $P < 0.001$; * $P < 0.05$; NS = not significant.

similar size (e.g., cup vs. can = 28.8%) than dissimilar size (e.g., cup vs. plate = 6.9%). Responses with device off (Fig. 14B) suggested a tendency to respond cup or bowl when uncertain, irrespective of the size or actual object.

The verbal localization ability for each of the nine object positions was also examined as response matrices, for data pooled from all time points (Supplementary Fig. S1). Response accuracy with the device on was greatest for objects located in the center row (80.0%–86.4%). Confusion was most often between adjacent rows or columns. For example, objects located in the back row were often reported as being in the center row, particularly for larger objects (i.e., plate and placemat) because their edges were closer to the cell boundary. Moreover, objects in the back row were the most difficult to identify (see object response matrices per row) (Supplementary Fig. S2).

To assess any effect of camera mount position on localization accuracy, we examined the reported azimuth per subject (Supplementary Fig. S3). The sole participant with a left-mounted camera (subject S1) had no detectable bias in reported azimuth. Two subjects with right-mounted cameras (subjects S2 and

S3) had higher localization accuracy for objects placed to the left and some confusion between center and right. The third subject with a right-mounted camera (subject S4) had equal accuracy for left and right and a small rightward bias for confused locations, sometimes responding center for objects at the left and right for objects in the center.

Obstacle Avoidance

Subjects were significantly more successful at detecting obstacles with the device on (Fig. 15A). However, the combination of head scanning and spatial assessment had an impact on walking speed; subjects were significantly slower at completing the task with the device on (Fig. 15B, all $P < 0.001$). Subjects S1, S2, and S4 contacted or collided with significantly fewer obstacles with the device on (Fig. 15C) ($P < 0.001$ for S1 and S2, $P < 0.01$ for S4). The percentage of trials with zero collisions or contact were significantly greater with the device on for S1 and S2 (both $P < 0.001$), and approached zero with the device off for all subjects (Fig. 15D).

Correlations between task performance and obstacle type or position were examined (Supplementary

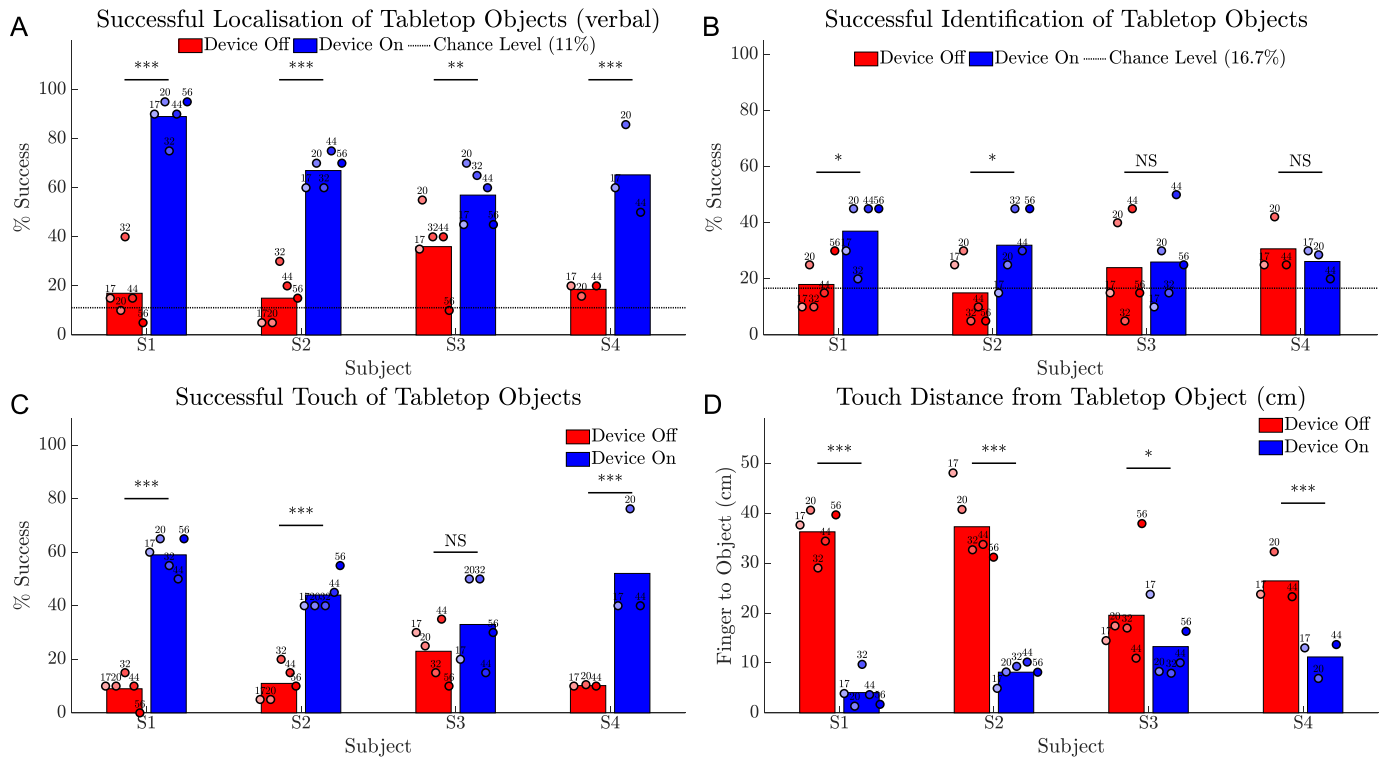


Figure 13. Results for the tabletop search task comparing device on (*blue*) versus device off (*red*). **(A)** Success rate (%) for verbally indicating object location on a 3×3 grid. **(B)** Success rate (%) for identifying object type (1 of 6). **(C)** Success rate (%) for contacting the object. **(D)** Distance from fingertip to object including successful touches. Chance level is indicated as a *horizontal dotted line* in **(A)** and **(B)**. Circles show the average of 20 trials at each time point, shaded progressively darker for later dates and labelled with week number. The height of the bar is each subject's average across all time points. Statistical significance of within-subject comparisons is shown; *** $P < 0.001$; ** $P < 0.01$; * $P < 0.05$; NS = not significant.

Fig. S4). The detection rate with the device on was poorest for the small wastepaper basket (ground) and small box (hanging). A decreased detection rate was observed for the large wastepaper basket when in the left of center location. Overall, the contact rate was highest for obstacles in the center location, principally because subjects started each trial aligned with this position. The contact rate for the center location was highest for wider ground-based obstacles, short pole (device on, 65%; device off, 91.4%) and large wastepaper basket (device on, 55.6%; device off, 95.9%), suggesting insufficient estimation of object boundaries when navigating past these wider obstacles.

The obstacle detection rate versus location and the contact rate versus location were examined per subject to again assess the effect of camera-mount position (Supplementary Fig. S5). Subjects S1 and S2 had no directional bias for detection rate, although their contact rate was higher for obstacles on the right. Subject S3 detected obstacles at the left more than those at the right. Subject S4 detected obstacles at the right more than those at the left.

Linear regression analyses to examine within-subject changes in performance over the study for the functional assessments did not reach significance in any comparisons.

Quality-of-Life Assessments

The FLORA assessments showed that orientation tasks (e.g., finding doorways) became easier with the device on over time, trending toward moderate from difficult, whereas they remained mostly difficult with the device off (Fig. 16A). The ease of completing activities of daily living (e.g., locating items in a familiar environment) also trended over time toward moderate with the device on, and remaining difficult with device off (Fig. 16C). Mobility tasks (Fig. 16B) and social interactions (Fig. 16D) were rated as mostly difficult with the device on and off, although subjects S1 and S2 demonstrated improved social interactions (such as detecting a person approaching) with the device on at weeks 44 and 56, whereas subject S3 continued to find these tasks as difficult (weeks 17–44) to impossible (week 56). Refer to Supplementary Figure S6 for

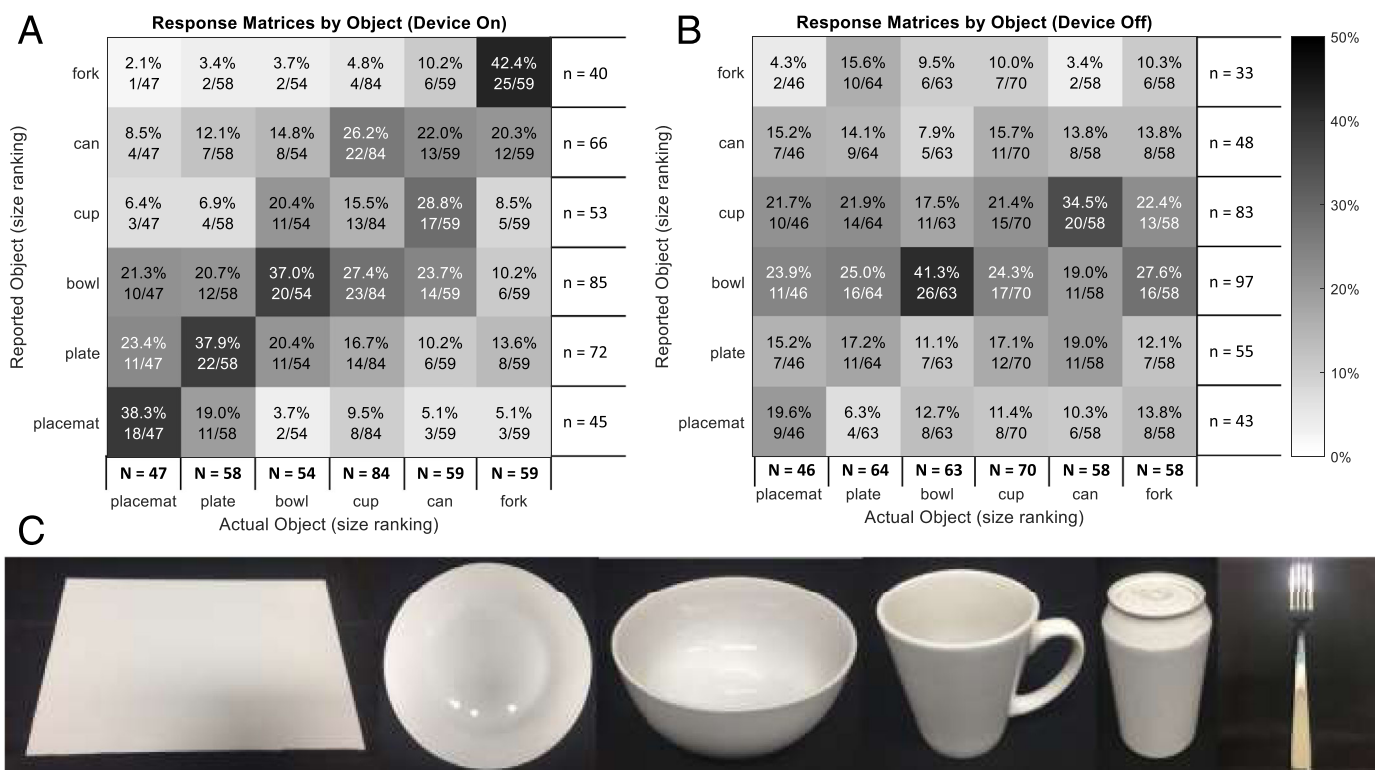


Figure 14. Response matrices for tabletop object identification pooled from all time points. **(A)** Comparisons with device on for reported object versus actual object demonstrate low scores for object identification but also clustering of responses according to the size of the actual object. **(B)** Comparisons with device off for reported object versus actual object. Cell text indicates incidence percent and fraction of actual object incidence. Row numerator totals (n) are the response incidence. Column numerator totals (N) are the total object incidence. **(C)** Photos of the objects used for tabletop search (from left): placemat, plate, bowl, cup, can, and fork.

a visualization of these data as stacked bar graphs. Subject S4 declined to complete the FLORA assessments.

The FLORA assessment also determined the degree to which the subject used their vision (i.e., the combination of residual vision and prosthetic vision) to complete each task (Figs. 16E–H). Completing the task with no vision implied that the subject relied on other senses for that task, such as auditory cues and proprioception. The contribution of vision to task performance was more with device on than with device off for mobility, activities of daily living, and social interactions (Figs. 16F–H) at weeks 20 to 56. Visual orientation (Fig. 16E) was the only task category in which subjects seemed to be equally likely to use prosthetic vision (device on) and residual vision (device off). Regular attempts and training on these tasks throughout the study, both with and without an orientation and mobility specialist, is likely to have contributed equally to the device on and device off improvements.

The scores for the emotional well-being component of the IVI-VLV were stable and did not differ from presurgery for three of the four subjects (Fig. 17A),

with a decrease for subject S4 being closely coupled with an increase in their Patient Health Questionnaire-9 score (not shown). An independent psychologist worked with this subject to address psychosocial stressors that were not study related. Scores for the three remaining subjects suggested they were well adjusted to their vision loss, with the impact of this on activities of daily living, mobility, and safety ranging from a little of the time to not at all (Fig. 17B). Device logs indicated that the frequency of at-home use for subjects S1 to S3 was every 2 to 3 days on average, for 2.3 ± 1.9 hours each instance. Subject S4 used the device on six occasions for a maximum of half an hour each instance.

Anecdotal Experiences

All subjects are able to use the device to localize the presence of light and detect whether a lightbulb is on or off. Three of four subjects are able to use the device to successfully sort laundry items into light and dark colors. Subjects report greater confidence in navigation, exhibited as a decreased tendency to stretch hands out when navigating through doorways in the home

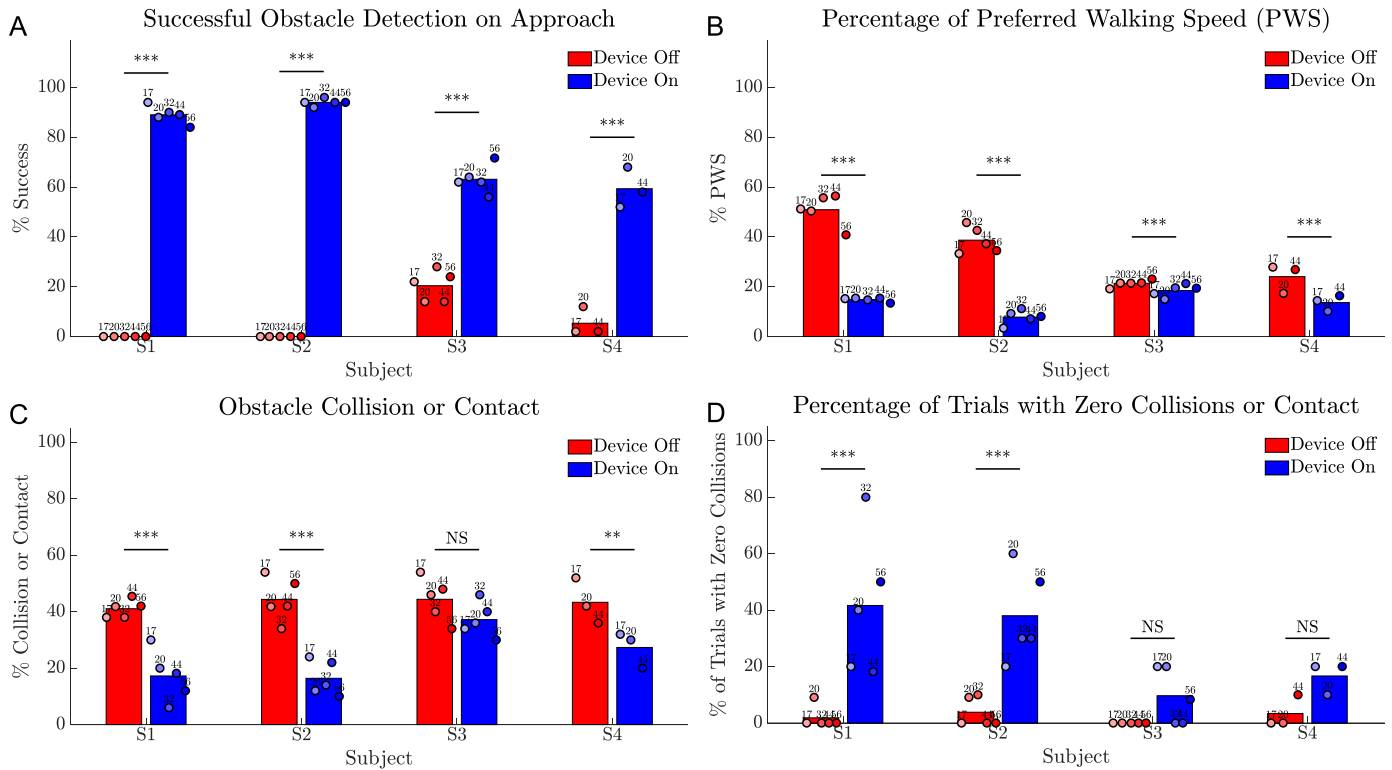


Figure 15. Results for the obstacle avoidance task comparing device on (blue) versus device off (red). (A) Success rate (%) for verbally indicating object location on approach. (B) Walking speed for each trial, expressed as percent of preferred walking speed (PWS). (C) Collision rate (%) for each trial. (D) Percent of trials with zero collisions or contact. Circles show the average of 10 trials at each time point, shaded progressively darker for later dates and labelled with week number. The height of the bar is each subject's average across all time points. Statistical significance of within-subject comparisons is shown; *** $P < 0.001$; ** $P < 0.01$; NS = not significant.

and an improved ability to avoid known obstacles such as a park bench in their local park or an unexpected vehicle parked across the footpath.

Overall, subjects have demonstrated an ability to count a series of people standing in a row, track a person walking, and develop strategies to decipher distance to obstacles and waypoints for navigating a known route.

Combining subject self-reports with the FLORA quality-of-life assessments, the independent examiner confirmed a positive impact of the retinal prosthesis on daily life for all subjects at all time points, with the sole exception of one neutral experience recorded for subject S3 at week 20.

Discussion

In this interim assessment of the safety and efficacy of the Bionic Vision Technologies Generation 2 device, we have confirmed that the surgical procedure is

safe, the electrode array remained in position under the macula, and the device was able to provide functional benefits in all four subjects. The electrode array was well tolerated by the eye and 98% of all electrodes remained functional at 56 weeks after switch on.

The main advantage with a suprachoroidal device is the safety, stability, and ease of the surgical approach, with no device-related SAEs recorded for the four subjects in this study or the three subjects in our previous prototype trial,⁸ as well as the demonstrable device efficacy in all subjects. The devices have been stable mechanically, with minimal lateral movement (maximum of 252 μm , which is 25% of one electrode diameter), some rotation (maximum 17°), and no signs of extrusion or retinal trauma.

As we have noted previously,⁸ a mild subretinal hemorrhage is an expected adverse event of this surgical approach (nonserious). Two of the four subjects exhibited a small trace of subretinal hemorrhage that cleared spontaneously within 2 weeks. The remainder of the surgery-related adverse events were all expected

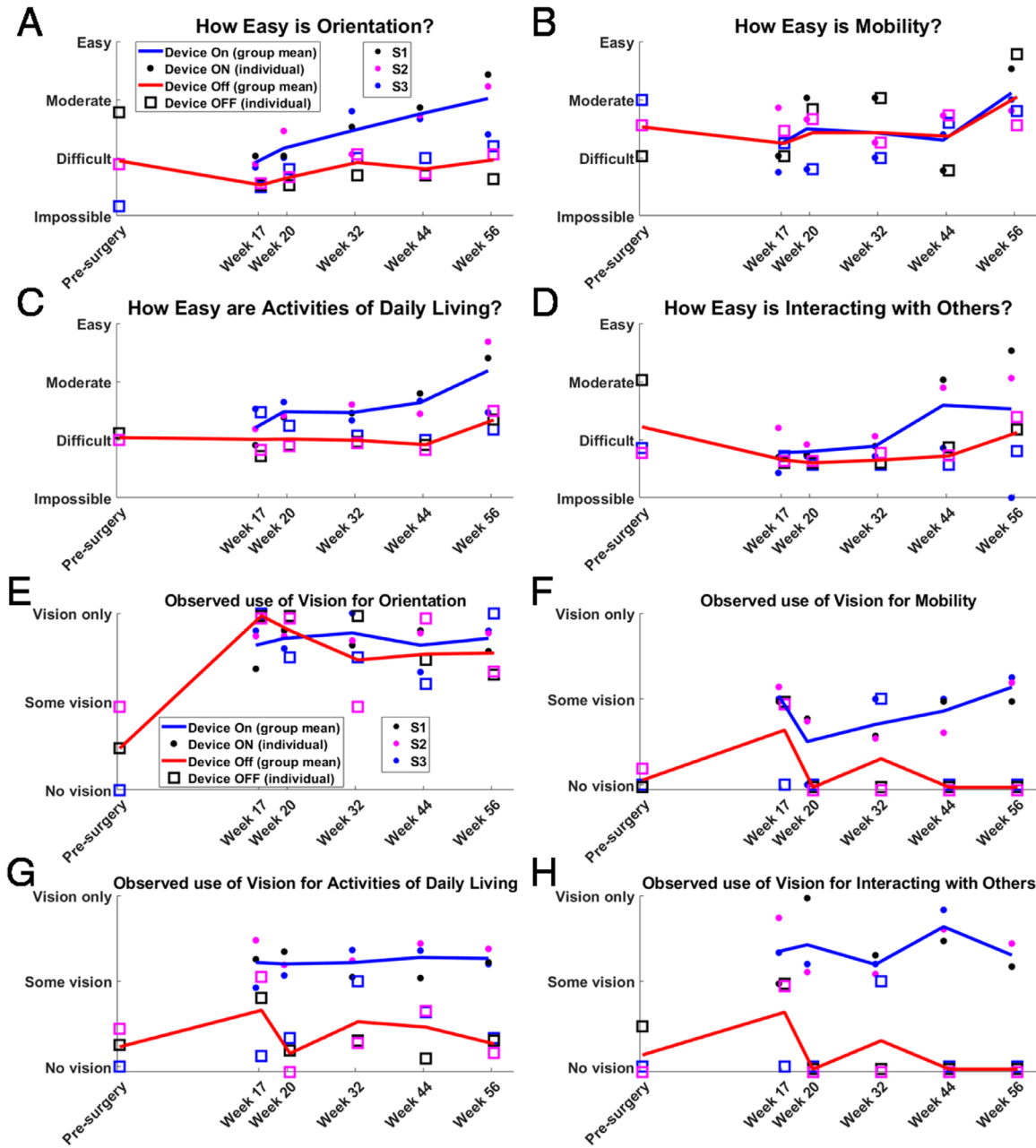


Figure 16. Group means and subject means for FLORA in four task categories: (A) orientation, (B) mobility, (C) activities of daily living, and (D) interacting with others. (E–H) The relative contribution of vision (with respect to other senses) was determined for these same tasks. One subject is excluded from this analysis (see text). Group averages are shown as blue lines (device on) and red lines (device off). Subject averages are shown as circles (device on) and squares (device off). The color key for individual subject week data is described in the legend of (A) and (E).

events: inflammation and tenderness, mild pain, and one instance of raised intraocular pressure in response to topical steroids.

The surgical procedures required for epiretinal and subretinal device placement are complex. The most common epiretinal device, the Argus II (Second Sight Medical Products), requires a pars plana vitrectomy and device insertion through a sclerotomy.³¹ The

placement of subretinal devices, such as the Alpha AMS (Retina Implant AG, Reutlingen, Germany) and PRIMA (Pixium Vision, Paris, France), require the additional steps of creation of a subretinal bleb and retinotomy to introduce the device.^{6,32} The incidence of SAEs related to these surgeries can include conjunctival and scleral erosions,^{6,31,33} retinal detachment,^{6,32,33} hypotony,^{31,34} and endophthalmi-

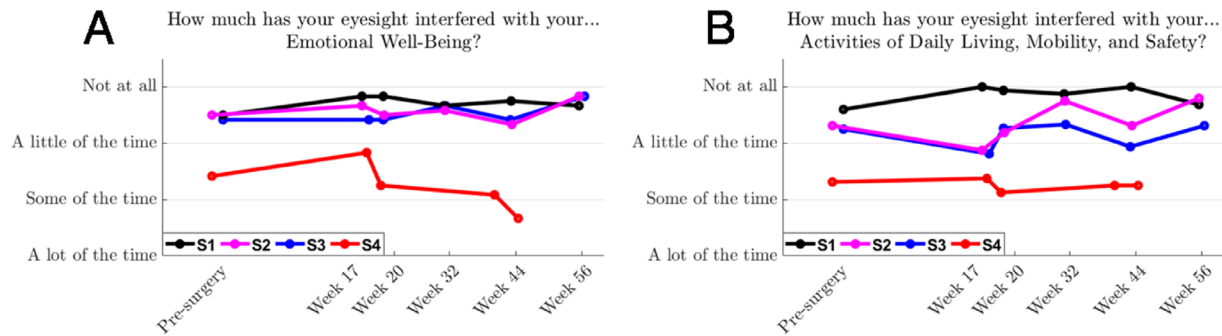


Figure 17. Subjects reported on the Impact of Vision Impairment (IVI-VLV) on their (A) emotional well-being and (B) activities of daily living, mobility, and safety in the month before each assessment. Subject averages are shown as *solid lines*. Assessments for subject S4 were markedly influenced by external stressors that were unrelated to the device or the study.

tis.³¹ Other human studies using suprachoroidal⁸ and intrascleral¹⁰ retinal prostheses show no evidence of intraocular SAEs, aside from iridocyclitis in the intrascleral subjects that resolved with a change in the stimulation parameters.

In contrast with our previous study, where we reported that increases in the electrode-to-retina distances were correlated with increases in perceptual threshold,¹⁶ the average thresholds for two of the four subjects in the present study decreased over time (Fig. 8B). The rate of electrode-to-retina increases after postoperative recovery (Fig. 8A) are less steep than for our 2012–2014 study,⁸ so it is possible that rate of increase is affected by choice of stimulation parameters. The previous study used stimulation rates up to 400 pulses per second and charge levels up to 447 nC,¹⁶ although the present study limited stimulation rates to 50 pulses per second and a charge limit of 250 nC per electrode (Nayagam DAX, et al. IOVS 2017;58:ARVO E-Abstract 4204). A further difference in the Generation 2 device is the increase in electrode diameter from 0.6 mm to 1.0 mm, which had the effect of decreasing the impedance of the electrode-to-tissue interface and safely decreasing the stimulation charge density. As the spread of stimulation current increases with electrode diameter, the perceptual threshold using larger electrodes is expected to be less sensitive to the electrode-to-retina distance.¹⁸

Although we were able to generate visual percepts in all four subjects within a safe charge limit, it was necessary to use ganged electrode pairs to safely produce percepts at peripheral locations because the required charge levels were higher than for electrode locations near the fovea. Subjects reported phosphene at the peripheral locations as being ill-defined and less focal. Ahuja and Behrend¹⁸ reported a relationship in epiretinal Argus II recipients between increasing foveal eccentricity and increasing charge requirements,

consistent with a corresponding decrease in ganglion cell density.³⁵ The extent of retina subtended by the suprachoroidal electrodes (excluding return electrodes) is approximately $38^\circ \times 28^\circ$ ¹³ (vs. approximately $11^\circ \times 19^\circ$ for the epiretinal Argus II³⁶ and approximately 15° on the diagonal for the subretinal Alpha AMS⁶); however, the maximum electrode eccentricity that produced a phosphene within the safety limits in this cohort was 25° from the fovea (Fig. 8C). The increased charge requirement observed for electrodes at peripheral locations is expected and consistent with lower ganglion cell density and greater degeneration of the retinal network.³⁷

The secondary efficacy outcomes clearly showed an overall positive effect of device use on common visual tasks in controlled environments as well as in the real-world setting. All subjects were significantly more accurate in the square localization task with the device on, with subject averages for error ranging from 9.2° to 11.9° . These results compare favorably with the reported accuracy of approximately 8° on average for 27 Argus II recipients.³⁸ The 1-year outcomes with a 49-channel suprachoroidal–transretinal device (Nidek Co., Tokyo, Japan) demonstrated a benefit of device on for one of three recipients (with best accuracy of approximately 8°).¹⁰

In a screen-based motion discrimination task with Argus II subjects, 54% of 28 subjects had a smaller mean error with device on than device off (at speeds up to 31.6°/s).³⁹ The Argus II studies differed from the four-alternative forced choice task in the present study: the moving bar stimuli in the Argus II studies were randomized into 1 of 360 directions, and subjects were required to respond within 15° of the stimulus direction by tracing the perceived direction on a touchscreen. In the present study, the motion discrimination performance for the suprachoroidal recipients was at similar levels; two of four subjects, S1 and S2, were able

to exceed the 62.5% pass criterion at 7, 15, and 30°/s. The marked decrease in performance for all subjects in the scrambled condition suggests that, to varying degrees, subjects were able to perceive spatial (retinotopic) information and prioritized this above head-directed gaze position when completing the tasks. This decrease in performance with the scrambled condition was more profound than in the square localization task, because the latter can be achieved with head-directed scanning (albeit with an offset error arising from the scrambled map). Although motion discrimination can be achieved with head-directed gaze at lower speeds, discrimination at higher speeds (e.g., 30°/s) requires retinotopic information.⁴⁰

We have recently published on our findings of a relationship between directional confusion in the motion discrimination task and the surgical position of the electrode array in the mediolateral and inferior–superior dimensions.⁴⁰ Additionally, naturalistic smooth pursuit eye movements, congruent with stimulus direction, were noted for subjects S1 and S2.⁴⁰ These same two subjects were more successful at spatial discrimination (0.033 cpd on the basic grating acuity assessment), indicating a probable association between successful motion discrimination and spatial discrimination. Motion discrimination is also possible with the Alpha IMS and AMS subretinal devices, with one exceptional recipient able to discriminate motion up to 35°/s (and grating acuity of 3.3 cpd), but otherwise only 18% to 21% of recipients passing the motion task at any speed.^{41,42} Despite the limited spatial acuity of relatively large suprachoroidal electrodes, it seems intuitive that the larger area of retina covered would provide a spatiotemporal benefit, allowing recipients to observe the progression of moving stimuli for a longer time period across a larger field-of-view.

The tabletop task in the present study combined size and depth discrimination with visual search and reaching accuracy. Localization and touch accuracy were significantly better with the device on, albeit with some depth confusion between the center and back rows (Supplementary Fig. S1), which could be improved with the inclusion of a stereo depth camera (Sadeghi R, et al. IOVS 2019;60:ARVO E-Abstract 4975).⁴³ Additionally, two subjects in this study reported physical difficulty when reaching for the back row in the tabletop task and the upper regions of the screen in the square localization task. There was also some mild confusion on the horizontal plane (Supplementary Fig. S3). Two subjects (S2 and S3) demonstrated greater accuracy for objects placed at the left than the right (Supplementary Fig. S3). This post hoc analysis has some limitations as the randomization of object location was not balanced, but the observed

error incidence is sufficiently high that this bias would remain if further successful (or unsuccessful) trials were conducted. The camera mount position was at the right-sided mount position for these subjects (Table 1); thus, the oblique head angle required to detect objects at the left is likely to have provided a more obvious proprioceptive feedback of object position. Behavioral confounds in reaching tasks, including compromised performance for eccentric targets, have been reported previously.⁴⁴ Object identification responses in the tabletop task were clustered according to object size, revealing an ability for the device to provide size discrimination (Fig. 14A). Previous reports of object identification ability in Argus II subjects were $32.8 \pm 15.7\%$ with the device on, improving to $41.4 \pm 17.7\%$ when black masking was used to enhance edge contrast (Luo YH, et al. IOVS 2014;55:ARVO E-Abstract 1834). Tabletop tasks have also been conducted with Alpha IMS/AMS recipients, with object identification being the most challenging aspect.^{7,42,45,46} Last, size discrimination has been assessed with the 49-channel suprachoroidal–transretinal device, comparisons between a rice bowl and a pair of chopsticks were significantly better with the device on for one of three recipients.¹⁰ In all, tabletop performance in the present study compares favorably with other retinal prosthesis studies.

A key quality-of-life benefit for visual prosthesis recipients is improvement in orientation and mobility. These attributes were demonstrated to be positive outcomes in controlled functional vision tasks (modified door task, obstacle avoidance) as well as in real-world settings (FLORA). All subjects were more successful with the device on at touching the target in the modified door task, with subject averages for three subjects exceeding 70%. Unsuccessful trials included near misses; subject averages for touch distance were only 4.8 to 29.5 cm away from the target with the device on. This compares favorably to mean task success of 50% in Argus II recipients ($n = 28$) at 12 months after implantation.⁴⁷ Improvements in mobility toward a target have not yet been reported for other visual prostheses, although improvements in following a white line on the floor have been reported for both the Argus II and Nidek suprachoroidal–transretinal devices.^{10,47}

Obstacle avoidance during navigation was assessed in this study using five randomly placed obstacles along a 20-m corridor. Walking speed (percentage of preferred walking speed) (Fig. 15B) was significantly slower with the device on, likely owing to increased visual scanning behavior and a sense of diminished visual field with the absence of their habitual mobility aid.⁴⁸ Obstacle detection was significantly better with the device on, although subjects contacted at

least one obstacle on average per traversal (compared with approximately two obstacles per traversal with the device off) (Fig. 15C). The higher incidence of contacts with wider ground-based obstacles suggest a challenge at correlating prosthetic camera-centric information with the relative body-centric position of the obstacle, which is presumed to occur with any combination of camera misalignment,⁴⁹ uncompensated eye movement,^{50,51} and an absence of depth cues.⁵² In contrast to the absence of directional bias for subject S4 in the tabletop task, his detection rate was much lower for obstacles at the left than at the right (Supplementary Fig. S5). The oblique gaze angle required to detect objects at the left with a right-sided camera position (Table 1) may have been difficult for this subject to achieve while walking. Similarly, low detection rates for subject S3 (Supplementary Fig. S5) may also indicate an impediment with head scanning in this task. Estimating angles and distances to visual landmarks has been described as “effortful and subject to inaccuracies” in Argus II subjects⁵³ and not reported in Alpha IMS/AMS subjects. Addressing these challenges remains a focus of visual prosthesis development.^{54,55}

Combining the observations across all laboratory-based assessments, the rank order of subject averages for localization results (square localization pointing error, modified door task touch distance, tabletop task, and touch distance) was consistent across all tasks—with subjects that performed well on one task also performing well in the others. Results for the motion discrimination and spatial discrimination tasks suggest that subjects S1 and S2 were able to perceive more readily spatial (retinotopic) information. Although the small number of subjects in this study limits our ability to relate outcomes directly to eye health, it may be that disease progression for the rod–cone RP variant (S1 and S2, Table 1) affects prosthetic visual function differently to the cone–rod RP variant (S3 and S4, Table 1), although any difference was not reflected conclusively in the phosphene thresholds (Fig. 8B) or maximal phosphene eccentricity (Fig. 8C). Variations in RP disease progression in Argus II recipients have been related previously to phosphene thresholds and functional outcomes.¹⁸

Outside the laboratory environment, the effect of the implant on subjects’ daily lives was assessed using the FLORA instrument, developed by Second Sight to evaluate the Argus II.²³ A study of 26 Argus II recipients at approximately 3 years after implantation demonstrated significantly improved device on performance on vision-related tasks, particularly tasks related to visual orientation.⁵⁶ Here, we also observed the strongest device benefit in visual orientation, with tasks that were previously evaluated as impossible to diffi-

cult requiring only moderate effort by week 56. Mobility tasks were observed to be difficult on average with the device on as well as with the device off and were affected by shadows and ambient light. This finding is in contrast with the Argus II study, where mobility tasks were rated on average as impossible with the device off, so the improvement to slightly above difficult at 2 years after implantation was significant.⁵⁶ Recent reports from a 17-patient postapproval Argus II study also seem to have a more modest rate of improvement, with the strongest task performance approaching moderate on average in the orientation domain.⁵⁷ Importantly, the suprachoroidal device does not obstruct incidental light from reaching the retina, so it was anticipated that both device on and device off performance could include contributions from residual light perception.

Activities of daily living tasks were improved with the device, such as determining whether room lights were on or off, navigating the home, and sorting light from dark laundry. These benefits were corroborated by the subjects’ spouses, with remarking that the subject was no longer stretching their hands out when navigating through doorways. Activities of daily living tasks were facilitated by the contrast information provided by the device, although the ambient lighting conditions (e.g., angle of light sources) proved important. Dagnelie et al.⁵⁸ reported a benefit of conducting laundry sorting tasks against a black-colored cloth, which increased contrast and was of a known color. Laundry sorting with the Alpha IMS/AMS may also be possible as discrimination of up to six levels of grayscale has reported.^{41,42}

Self-reported vision-related quality of life was monitored using the IVI-VLV instrument.²⁴ This assessment differs from other instruments that are aimed at populations with mild to moderate vision loss, because patients suitable for retinal prostheses typically do not perform many of the activities queried by such instruments.⁵⁶ Before the availability of the IVI-VLV, improvements in quality of life for 30 Argus II recipients were assessed using the Vision and Quality of Life Index,⁵⁹ but found no significant difference in the composite scores between presurgical baseline and follow-up.⁶⁰ Similarly, the IVI-VLV data in the present study showed that emotional well-being was not impacted by device implantation or use.

A limitation of the study is that only four patients were examined and the study is ongoing. However, this interim study report has shown that the 44-channel retinal prosthesis can be implanted safely in the suprachoroidal space, with no SAEs recorded for any subjects and 97% of electrodes still functional to date. The interim outcome data demonstrate that the prosthesis provides significant improvements

in functional vision, activities of daily living, and observer-rated quality of life. The safety and efficacy of the suprachoroidal approach make it an excellent option to improve functional vision in late-stage RP.

Acknowledgments

The authors thank the following people for their respective contributions: the surgical staff at the Royal Victorian Eye and Ear Hospital; Rebecca Dengate, Nariman Habili, Madhura Korikkar, Jason Leavens, Ceara McGowan, Jeremy Oorloff, Darien Pardinas Diaz, Adele Scott, Ashley Stacey, and Godofredo Timbol, for their assistance with device development; Rosie Dawkins for assistance with follow-up eye health checks; Stefan Czyniewski and Mobius Medical for clinical trial oversight; Tamara Brawn, Georgia Giannakis, Brian Gordon, and Bionic Vision Technologies; Second Sight Medical Products for providing the FLORA instrument; and Michael Bach for providing modifications to the Basic Grating Acuity (BaGA) test program.

Supported by the National Health and Medical Research Council (NHMRC) Grant 1082358 (PJA; Canberra, ACT, Australia) and Bionic Vision Technologies Pty Ltd (Australia). The Bionics Institute and the Centre for Eye Research Australia wish to acknowledge the support of the Victorian Government through its Operational Infrastructure Support Program (Victoria, Australia), and for generous support from the estate of the late Brian Entwisle.

Disclosure: **M.A. Petoe**, BI (P), BVT (F,R); **S.A. Titchener**, BVT (F); **M. Kolic**, BVT (F,R); **W.G. Kentler**, BVT (F); **C.J. Abbott**, BVT (F,R); **D.A.X. Nayagam**, BI (P), BVT (F); **E.K. Baglin**, BVT (F,R); **J. Kvensakul**, BVT (F); **N. Barnes**, ANU (P), BVT (F); **J.G. Walker**, BVT (F); **S.B. Epp**, BVT (F); **K.A. Young**, BVT (F); **L.N. Ayton**, none; **C.D. Luu**, BVT (F); **P.J. Allen**, BVT (F), CERA (P)

See the appendix for the members of the Bionics Institute and Centre for Eye Research Australia Retinal Prosthesis Consortium.

References

- Dias MF, Joo K, Kemp JA, et al. Molecular genetics and emerging therapies for retinitis pigmentosa: basic research and clinical perspectives. *Prog Retin Eye Res.* 2018;63:107–131.
- Russell S, Bennett J, Wellman JA, et al. Efficacy and safety of voretigene neparvovec (AAV2-hRPE65v2) in patients with RPE65-mediated inherited retinal dystrophy: a randomised, controlled, open-label, phase 3 trial. *Lancet.* 2017;390:849–860.
- Ayton LN, Barnes N, Dagnelie G, et al. An update on retinal prostheses. *Clin Neurophysiol.* 2020;131:1383–1398.
- Luo YH-L, da Cruz L. The Argus II retinal prosthesis system. *Prog Retin Eye Res.* 2016;50:89–107.
- Palanker D, Le Mer Y, Mohand-Said S, Muqit M, Sahel JA. Photovoltaic restoration of central vision in atrophic age-related macular degeneration. *Ophthalmology.* 2020;127:1097–1104.
- Edwards TL, Cottrill CL, Xue K, et al. Assessment of the electronic retinal implant Alpha AMS in restoring vision to blind patients with end-stage retinitis pigmentosa. *Ophthalmology.* 2018;125:432–443.
- Stingl K, Bartz-Schmidt KU, Besch D, et al. Artificial vision with wirelessly powered subretinal electronic implant alpha-IMS. *Proc R Soc B Biol Sci.* 2013;280:20130077.
- Ayton LN, Blamey PJ, Guymer RH, et al. First-in-human trial of a novel suprachoroidal retinal prosthesis. *PLoS One.* 2014;9:e115239.
- Villalobos J, Nayagam DAX, Allen PJ, et al. A wide-field suprachoroidal retinal prosthesis is stable and well tolerated following chronic implantation. *Invest Ophthalm Vis Sci.* 2013;54:3751–3762.
- Fujikado T, Kamei M, Sakaguchi H, et al. One-year outcome of 49-channel suprachoroidal-transretinal stimulation prosthesis in patients with advanced retinitis pigmentosa. *Invest Ophthalm Vis Sci.* 2016;57:6147–6157.
- Ayton LN, Apollo NV, Varsamidis M, Dimitrov PN, Guymer RH, Luu CD. Assessing residual visual function in severe vision loss. *Invest Ophthalm Vis Sci.* 2014;55:1332–1338.
- Klein M, Birch D. Psychophysical assessment of low visual function in patients with retinal degenerative diseases (RDDs) with the Diagnosys full-field stimulus threshold (D-FST). *Doc Ophthalmol.* 2009;119:217–224.
- Dacey DM, Petersen MR. Dendritic field size and morphology of midget and parasol ganglion cells of the human retina. *P Natl Acad Sci USA.* 1992;89:9666–9670.
- Barnes N, Scott AF, Lieby P, et al. Vision function testing for a suprachoroidal retinal prosthesis: effects of image filtering. *J Neural Eng.* 2016;13:15.

15. Saunders AL, Williams CE, Heriot W, et al. Development of a surgical procedure for implantation of a prototype suprachoroidal retinal prosthesis. *Clin Exp Ophthalmol*. 2014;42:665–674.
16. Shivdasani MN, Sinclair NC, Dimitrov PN, et al. Factors affecting perceptual thresholds in a suprachoroidal retinal prosthesis. *Invest Ophthalmol Vis Sci*. 2014;55:6467–6481.
17. Ayton LN, Rizzo JF, III, Bailey IL, et al. Harmonization of outcomes and vision endpoints in vision restoration trials: recommendations from the International HOVER Taskforce. *Transl Vis Sci Technol*. 2020;9:25.
18. Ahuja AK, Behrend MR. The Argus II retinal prosthesis: factors affecting patient selection for implantation. *Prog Retin Eye Res*. 2013;36:1–23.
19. Petoe MA, McCarthy CD, Shivdasani MN, et al. Determining the contribution of retinotopic discrimination to localization performance with a suprachoroidal retinal prosthesis. *Invest Ophthalmol Vis Sci*. 2017;58:3231–3239.
20. Bach M, Wilke M, Wilhelm B, Zrenner E, Wilke R. Basic quantitative assessment of visual performance in patients with very low vision. *Invest Ophthalmol Vis Sci*. 2010;51:1255–1260.
21. Humayun MS, Dorn JD, da Cruz L, et al. Interim results from the international trial of Second Sight's visual prosthesis. *Ophthalmology*. 2012;119:779–788.
22. Finger RP, McSweeney SC, Deverell L, et al. Developing an instrumental activities of daily living tool as part of the low vision assessment of daily activities protocol. *Invest Ophthalmol Vis Sci*. 2014;55:8458–8466.
23. Geruschat DR, Flax M, Tanna N, et al. FLORA: phase I development of a functional vision assessment for prosthetic vision users. *Clin Exp Optom*. 2015;98:342–347.
24. Finger RP, Tellis B, Crewe J, Keeffe JE, Ayton LN, Guymer RH. Developing the Impact of Vision Impairment-Very Low Vision (IVI-VLV) Questionnaire as part of the LoVADA protocol. *Invest Ophthalmol Vis Sci*. 2014;55:6150–6158.
25. Kroenke K, Spitzer RL, Williams JB. The PHQ-9: validity of a brief depression severity measure. *J Gen Intern Med*. 2001;16:606–613.
26. Wittkowski KM. Friedman-type statistics and consistent multiple comparisons for unbalanced designs with missing data. *J Am Stat Assoc*. 1988;83:1163–1170.
27. R Core Team. *R: a language and environment for statistical computing*. Vienna, Austria: R Foundation for Statistical Computing; 2020. Available at: <https://www.R-project.org>.
28. Wittkowski KM, Song T. *muStat: Prentice rank sum test and McNemar test. R package version 1.7.0*. Vienna, Austria: R Foundation for Statistical Computing; 2012. Available at: <https://CRAN.R-project.org/package=muStat>.
29. Conover WJ. *Practical nonparametric statistics*. New York: John Wiley & Sons; 1998.
30. Holm S. A simple sequentially rejective multiple test procedure. *Scand J Stat*. 1979;6:65–70.
31. Ghodasra DH, Chen A, Arevalo JF, et al. Worldwide Argus II implantation: recommendations to optimize patient outcomes. *BMC Ophthalmol*. 2016;16:52.
32. Muqit MMK, Hubschman JP, Picaud S, et al. PRIMA subretinal wireless photovoltaic microchip implantation in non-human primate and feline models. *PLoS One*. 2020;15:e0230713.
33. Schaffrath K, Schellhase H, Walter P, et al. One-year safety and performance assessment of the Argus II retinal prosthesis: a postapproval study. *Jama Ophthalmol*. 2019;137:896–902.
34. Luo YH-L, Zhong JJ, da Cruz L. The use of Argus II retinal prosthesis by blind subjects to achieve localisation and prehension of objects in 3-dimensional space. *Graefes Arch Clin Exp Ophthalmol*. 2014;253:1907–1914.
35. Curcio CA, Allen KA. Topography of ganglion cells in human retina. *J Comp Neurol*. 1990;300:5–25.
36. Yue L, Weiland JD, Roska B, Humayun MS. Retinal stimulation strategies to restore vision: fundamentals and systems. *Prog Retin Eye Res*. 2016;53:21–47.
37. Jones BW, Pfeiffer RL, Ferrell WD, Watt CB, Marmor M, Marc RE. Retinal remodeling in human retinitis pigmentosa. *Exp Eye Res*. 2016;150:149–165.
38. Ahuja AK, Dorn JD, Caspi A, et al. Blind subjects implanted with the Argus II retinal prosthesis are able to improve performance in a spatial-motor task. *Br J Ophthalmol*. 2011;95:539–543.
39. Dorn JD, Ahuja AK, Caspi A, et al. The Detection of motion by blind subjects with the epiretinal 60-electrode (Argus II) retinal prosthesis. *JAMA Ophthalmol*. 2013;131:183–189.
40. Titchener SA, Kvensakul J, Shivdasani MN, et al. Oculomotor responses to dynamic stimuli in a 44-channel suprachoroidal retinal prosthesis. *Transl Vis Sci Technol*. 2020;9:31–31.
41. Stingl K, Bartz-Schmidt KU, Besch D, et al. Subretinal visual implant Alpha IMS – clinical trial interim report. *Vision Res*. 2015;111:149–160.
42. Stingl K, Schippert R, Bartz-Schmidt KU, et al. Interim results of a multicenter trial with the new

- electronic subretinal implant Alpha AMS in 15 patients blind from inherited retinal degenerations. *Front Neurosci.* 2017;11:445.
43. Kartha A, Sadeghi R, Barry MP, et al. Prosthetic visual performance using a disparity-based distance-filtering system. *Transl Vis Sci Technol.* 2020;9:27–27.
 44. Endo T, Kanda H, Hirota M, Morimoto T, Nishida K, Fujikado T. False reaching movements in localization test and effect of auditory feedback in simulated ultra-low vision subjects and patients with retinitis pigmentosa. *Graefes Arch Clin Exp Ophthalmol.* 2016;254:947–956.
 45. Stingl K, Bach M, Bartz-Schmidt KU, et al. Safety and efficacy of subretinal visual implants in humans: methodological aspects. *Clin Exp Optom.* 2013;96:4–13.
 46. Wilke R, Bach M, Wilhelm B, Durst W, Trauzettel-Klosinski S, Zrenner E. Testing visual functions in patients with visual prostheses. *Artificial Sight.* New York: Springer; 2007;91–110.
 47. da Cruz L, Dorn JD, Humayun MS, et al. Five-year safety and performance results from the Argus II Retinal prosthesis system clinical trial. *Ophthalmology.* 2016;123:2248–2254.
 48. Finger RP, Ayton LN, Deverell L, et al. Developing a very low vision orientation and mobility test battery (O&M-VLV). *Optom Vis Sci.* 2016;93:1127–1136.
 49. Barry MP, Dagnelie G. Hand-camera coordination varies over time in users of the Argus II retinal prosthesis system. *Front Syst Neurosci.* 2016; 10:41.
 50. Sabbah N, Authie CN, Sanda N, Mohand-Said S, Sahel JA, Safran AB. Importance of eye position on spatial localization in blind subjects wearing an Argus II retinal prosthesis. *Invest Ophthalmol Vis Sci.* 2014;55:8259–8266.
 51. Turano KA, Geruschat DR, Baker FH, Stahl JW, Shapiro MD. Direction of gaze while walking a simple route: persons with normal vision and persons with retinitis pigmentosa. *Optom Vis Sci.* 2001;78:667–675.
 52. McCarthy C, Walker JG, Lieby P, Scott A, Barnes N. Mobility and low contrast trip hazard avoidance using augmented depth. *J Neural Eng.* 2014;12:016003.
 53. Garcia S, Petrini K, Rubin GS, Da Cruz L, Nardini M. Visual and non-visual navigation in blind patients with a retinal prosthesis. *PloS One.* 2015;10:e0134369.
 54. Caspi A, Roy A, Wuyyuru V, et al. Eye movement control in the Argus II retinal-prosthesis enables reduced head movement and better localization precision. *Invest Ophthalmol Vis Sci.* 2018;59:792–802.
 55. Titchener SA, Shivdasani MN, Fallon JB, Petoe MA. Gaze compensation as a technique for improving hand-eye coordination in prosthetic vision. *Transl Vis Sci Technol.* 2018;7:2.
 56. Geruschat DR, Richards TP, Arditì A, et al. An analysis of observer-rated functional vision in patients implanted with the Argus II retinal prosthesis system at three years. *Clin Exp Optom.* 2016;99:227–232.
 57. Delyfer MN, Gaucher D, Mohand-Said S, et al. Improved performance and safety from Argus II retinal prosthesis post-approval study in France. *Acta Ophthalmol.* 2020, doi:10.1111/aos.14728. Online ahead of print.
 58. Dagnelie G, Christopher P, Arditì A, et al. Performance of real-world functional vision tasks by blind subjects improves after implantation with the Argus II retinal prosthesis system. *Clin Exp Ophthalmol.* 2017;45:152–159.
 59. Misajon R, Hawthorne G, Richardson J, et al. Vision and quality of life: the development of a utility measure. *Invest Ophthalmol Vis Sci.* 2005;46:4007–4015.
 60. Duncan JL, Richards TP, Arditì A, et al. Improvements in vision-related quality of life in blind patients implanted with the Argus II Epiretinal Prosthesis. *Clin Exp Optom.* 2017;100:144–150.

Appendix. The Bionics Institute and Centre for Eye Research Australia Retinal Prosthesis Consortium

For this publication, the Bionics Institute and Centre for Eye Research Australia Retinal Prosthesis Consortium consists of (in alphabetical order): Peter J. Blamey¹; Robert J. Briggs^{2,3}; Owen Burns¹; Dean Johnson; Lewis Karapanos^{4,5}; Hugh J. McDermott^{1,6}; Myra B. McGuinness^{4,7}; Rodney E. Millard¹; Peter M. Seligman^{1,6}; Robert K. Shepherd^{1,6}; Mohit N. Shivdasani^{1,8}; Nicholas C. Sinclair^{1,6}; Patrick C. Thien^{1,6}; Joel Villalobos^{1,6}; Chris E. Williams^{1,6,9}; Jonathan Yeoh^{4,10}

¹Bionics Institute, East Melbourne, Victoria, Australia

²Department of Otolaryngology, Royal Victorian Eye and Ear Hospital, Melbourne, Victoria, Australia

³Otolaryngology, Department of Surgery, University of Melbourne, Melbourne, Victoria, Australia

⁴Centre for Eye Research Australia, Royal Victorian Eye and Ear Hospital, Melbourne, Victoria, Australia

⁵Ophthalmology, Department of Surgery, University of Melbourne, Melbourne, Victoria, Australia

⁶Medical Bionics Department, University of Melbourne, Melbourne, Victoria, Australia

⁷Melbourne School of Population and Global Health, University of Melbourne, Victoria, Australia

⁸Graduate School of Biomedical Engineering, University of New South Wales, New South Wales, Australia

⁹Department of Pathology, University of Melbourne, St. Vincent's Hospital, Victoria, Australia

¹⁰Department of Ophthalmology, Royal Victorian Eye and Ear Hospital, Melbourne, Victoria, Australia